Author Manuscript

Author Manuscript

Author Manuscript

Author Manuscript

HHS Public Access

Author manuscript

J Med Chem. Author manuscript; available in PMC 2016 August 27.

Published in final edited form as:

J Med Chem. 2015 August 27; 58(16): 6589–6606. doi:10.1021/acs.jmedchem.5b00710.

Development of Selective Covalent Janus Kinase 3 Inhibitors

Li Tan[1,2,†], **Koshi Akahane**[3,†], **Randall McNally**[1,2], **Kathleen M. S. E. Reyskens**[4], **Scott B. Ficarro**[1,2], **Suhu Liu**[5], **Grit S. Herter-Sprie**[5], **Shohei Koyama**[5], **Michael J. Pattison**[4], **Katherine Labella**[5], **Liv Johannessen**[1,2], **Esra A. Akbay**[5], **Kwok-Kin Wong**[5], **David A. Frank**[5], **Jarrod A. Marto**[1,2], **Thomas A. Look**[3], **J. Simon C. Arthur**[4], **Michael J. Eck**[1,2], and **Nathanael S. Gray**[1,2,*]

[1]Department of Biological Chemistry and Molecular Pharmacology, Harvard Medical School, Boston, MA 02115 (USA)

[2]Department of Cancer Biology, Dana Farber Cancer Institute, Boston, MA 02215 (USA)

[3]Department of Pediatric Oncology, Dana Farber Cancer Institute, Boston, MA 02215 (USA)

[4]Division of Cell Signaling and Immunology, College of Life Sciences, University of Dundee, Dundee DD1 5EH (UK)

[5]Department of Medical Oncology, Dana Farber Cancer Institute, Boston, MA 02215 (USA)

Abstract

The Janus Kinases (JAKs) and their downstream effectors Signal Transducer and Activator of Transcription proteins (STATs) form a critical immune cell signaling circuit, which is of fundamental importance in innate immunity, inflammation and hematopoiesis and dysregulation is frequently observed in immune disease and cancer. The high degree of structural conservation of the JAK ATP binding pockets has posed a considerable challenge to medicinal chemists seeking to develop highly selective inhibitors as pharmacological probes and as clinical drugs. Here we report the discovery and optimization of 2,4-substituted pyrimidines as covalent JAK3 inhibitors that exploit a unique cysteine (Cys909) residue in JAK3. Investigation of structure-activity-relationship (SAR) utilizing biochemical and transformed Ba/F3 cellular assays resulted in identification of potent and selective inhibitors such as compounds **9** and **45**. A 2.9 Å co-crystal structure of JAK3 in complex with **9** confirms the covalent interaction. Compound **9** exhibited decent pharmacokinetic properties and is suitable for use *in vivo*. These inhibitors provide a set of useful tools to pharmacologically interrogate JAK3-dependent biology.

TOC image

*Correspondence: nathanael_gray@dfci.harvard.edu (NSG).

†These authors contributed equally.

Supporting Information Available: Figure S1–6; Table S1–4; Structures and spectral data of **14**–**64** and **66**–**85**; Complete KinomeScan profiling data of **9** and **45**. This material is available free of charge via the Internet at http://pubs.acs.org. X-ray coordinates and structure factors have been deposited in the Protein Data Bank. PDB accession code: 4Z16.

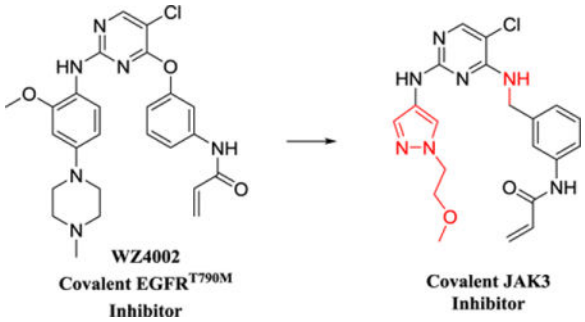

Keywords

JAK3; Covalent kinase inhibitors; Structure-based design; Structure-activity relationship; Drug discovery

Introduction

The Janus Kinases (JAKs) and their downstream effectors Signal Transducer and Activator of Transcription proteins (STATs) form a critical immune cell signaling circuit.[1] There are four JAK family members in mammals, JAK1, JAK2, JAK3 and tyrosine kinase 2 (TYK2), each of which can bind to distinct cytokines and/or growth factor receptors. As the receptors that act upstream of JAKs are dimeric or multimeric, more than one JAK molecule is recruited to each receptor. Ligand binding to the receptor results in a conformation change that brings two JAK molecules close together allowing them to trans-phosphorylate and activate each other. Once active, JAKs catalyze the phosphorylation of tyrosine residues in the receptor allowing the recruitment of specific STATs which are in turn phosphorylated by the JAK. This promotes STAT dimerization which induces translocation to the nucleus and activation of gene regulatory programs.[2] JAK/STAT signaling is of fundamental importance in innate immunity, inflammation and hematopoiesis and dysregulation is frequently observed in immune disease and cancer.[3] The JAKs have been the subject of extensive drug discovery efforts and numerous small molecule ATP-competitive inhibitors have been developed including ruxolitinib (**1**, JAK1/2 inhibitor)[4] approved as an anti-myelofibrosis drug, tofacitinib (**2**, pan-JAK inhibitor)[5] approved for rheumatoid arthritis, and several others that are currently undergoing clinical investigation.[6] The high degree of structural conservation of the JAK ATP binding pockets has posed a considerable challenge to medicinal chemists seeking to develop highly selective inhibitors as pharmacological probes and as clinical drugs.[7]

Among the JAK family JAK3 exhibits predominant expression in the hematopoietic system in contrast to other JAKs which are broadly expressed in a variety of cell types.[2b] JAK3 is required for signaling by cytokines, including interleukin 2 (IL-2), IL-4, IL-7, IL-9, IL-15 and IL-21, that act via receptors that contain the common gamma chain (γ_c) cytokine receptor subunit.[8] In addition to the γ_c subunit, most of these receptors contain a second unique α subunit that determines cytokine specificity. In these receptors, JAK3 binds to the γ_c subunit and JAK1 to the α subunit. The IL-2 Receptor (IL-2R) and IL-15R are exceptions to this as they can form trimeric complexes through the recruitment of α and β chains. In this

Author Manuscript Author Manuscript Author Manuscript Author Manuscript

Author Manuscript Author Manuscript Author Manuscript Author Manuscript

case the β subunit binds JAK1; the α subunit, while involved in cytokine binding, does not directly bind to a JAK.[9] Signaling via the γ_c receptors is essential for the normal development and function of the immune system. Loss-of-function mutations in either γ_c or JAK3 in humans results in severe combined immunodeficiency caused by defective development of T- and NK cells. The role for JAK3 in T and natural killer (NK) cell development was subsequently confirmed by deletion of Jak3 in mice; JAK3 knockouts also lacked normal numbers of B cells indicating a more important role for JAK3 in B cell development in mice than in humans.[2b, 10] On the basis of JAK3's essential function in immune signaling and its restricted expression in hematopoietic tissues, JAK3 has been pursued as a target for the treatment of autoimmune and inflammatory diseases. JAK3 has also been explored as a potential anti-cancer target due to aberrant activation in several lymphoproliferative disorders;[11] for example, mutations in JAK3 have been found in leukemias such as T-cell acute lymphoblastic leukemia (T-ALL) and T-cell prolymphocytic leukemia (T-PLL).[12] The A572V activating mutation in the kinase domain of JAK3 was discovered in acute megakaryoblastic leukemia and natural killer/T-cell lymphoma, and has been demonstrated to be capable of forming tumors in mice.[13] Recently JAK3 mutations were also found to promote programmed death ligand 1 (PD-L1) induction in lung cancer cells an in the tumor immune microenvironments.[14]

The most obvious strategy to develop small-molecule JAK3 inhibitors is to target the catalytic ATP-binding site of the JAK3 kinase domain (JH1). Numerous ATP-competitive JAK3 inhibitors have been developed (Figure 1A).[15] Tofacitinib (**2**) was developed as a specific JAK3 inhibitor to prevent organ-transplant rejection but subsequent studies revealed that it is also a potent inhibitor of JAK1 and JAK2.[5, 16] The combination of compound **2**'s excellent potency, selectivity and pharmacological properties have made it a favored inhibitor to interrogate JAK kinase activity in numerous biological models.[13b, 17] In our efforts to develop a more selective Jak3 inhibitor, we noted that among JAK family members JAK3 is unique in having a cysteine residue at the gatekeeper-plus-7 (GK+7) position.[18] This residue is Cys909 in human JAK, and it is structurally equivalent to cysteine residues in epidermal growth factor receptor (EGFR) and Bruton's tyrosine kinase (BTK) that have been successfully targeted by covalent kinase inhibitors that are now approved drugs. Afatinib[19] (**6**) targets Cys797 in EGFR and ibrutinib[20] (**7**) targets Cys481 in BTK. We and others have also developed mutant-selective inhibitors of the drug-resistant EGFR T790M that react covalently with Cys797. WZ4002[21] (**8**) is a pyrimidine-based inhibitor with an acrylamide "warhead"[22] that potently inhibits EGFR T790M. Recently three other groups have also reported the development of covalent JAK3 inhibitors. In 2013 Winssinger et al. reported a covalent probe which selectively labeled JAK3, EGFR and ERBB2.[23] Taunton et.al reported the development of 'reversible-covalent' JAK3 inhibitors incorporating a cyanoacrylamide warhead which inhibited JAK3 in a biochemical kinase assay with an IC_{50} of 100 nM while sparing other JAKs up to a concentration of 10 μM.[24] Goedken et.al reported several tricyclic covalent JAK3 inhibitors with optimized inhibitors exhibiting biochemical IC_{50}'s of 7 nM, good kinome selectivity and confirmed covalent binding to Cys909 using kinetic and mass-spectrometry studies.[25] Here we report a medicinal campaign to derive potent disubstituted pyrimidine-based inhibitors that exploit an acrylamide electrophile to form a covalent bond to Cys909. Optimization was guided by

Author Manuscript Author Manuscript Author Manuscript Author Manuscript

cellular assays using Translocation ETS Leukemia protein (Tel)-JAK[26] fusion kinase transformed Ba/F3 cells that provided an efficient and reliable measure of the ability of compounds to inhibit JAK signaling in cellular context.

Results

Identification of Compound 9 as a Potent JAK3 Inhibitor

Amongst the 11 kinases that possess a cysteine at the GK+7 position only JAK3 and mitogen-activated protein kinase kinase 7 (MAP2K7) have a methionine gatekeeper, which is also present in the drug-resistant $EGFR^{T790M}$ that is targeted by the pyrimidine-based inhibitor WZ4002 (**8**). Compound **8** is a much less potent inhibitor of cellular JAK3 kinase activity (JAK3 Kd = 150 nM, TEL-JAK3 Ba/F3 IC_{50} = 2.82 μM) compared to T790M EGFR ($EGFR^{L858R/T790M}$ Ba/F3 IC_{50} = 8 nM).[21] Through the syntheses of a small collection of analogs of **8** we discovered that relatively subtle changes could result in a dramatic improvement in JAK3 inhibitory potency relative to $EGFR^{T790M}$. For example, **9** where the ether linkage of **8** is replaced with an aminomethylene (-$NHCH_2$-) linkage resulted in a great improvement in JAK3 inhibition in a fixed time-point Z'-lyte enzymatic assay (Life Technology, SelectScreen, IC_{50} = 4.8 nM) (Scheme 1A).

To broadly assess its kinase selectivity, **9** was profiled against a diverse panel of 456 kinases (DiscoveRX, KinomeScan[27]) using an *in vitro* ATP-site competition binding assay at a concentration of 1.0 μM. Compound **9** exhibited good overall kinase selectivity with an S(5) selectivity score, defined as the percentage of kinases with scores less than 5 (S(5))[27b], of 0.02. The results suggested that **9** most potently inhibits JAK3 and identified fms-related tyrosine kinase 3 (FLT3) and several tyrosine protein kinase (TEC)-family kinases as being potential off-targets (Figure 2). Enzymatic assays using the Z'-lyte or LanthaScreen[28] formats confirmed enzymatic inhibition of FLT3 (IC_{50} = 13 nM), TTK protein kinase (TTK, IC_{50} = 49 nM), BLK proto-oncogene (BLK, IC_{50} = 157 nM) and tyrosine protein kinase TXK (TXK, IC_{50} = 36 nM). Compound **9** showed very low inhibition scores for other JAKs and wild-type (WT) EGFR, which is consistent with the over 180-fold higher IC_{50}s against JAK1, JAK2, TYK2 and $EGFR^{WT}$ (IC_{50}s = 896, 1050, > 10000 and 409 nM respectively). As BTK and ITK have important functions in B-cell and T-cell signaling pathways, we confirmed that compound **9** possesses over 165-fold higher IC_{50}s for BTK or ITK (IC_{50}s = 794 and 1070 nM respectively) (Table S1).

As enzymatic potencies sometimes do not translate into cellular inhibition, the ability of **9** to inhibit the proliferation of kinase-transformed Ba/F3 cells was evaluated. Ba/F3 cells are a murine pre-B cell that can readily be transformed with activated kinases to allow for growth in the absence of IL-3, and are frequently used to evaluate the activity of compounds against kinases of interest in a cellular context.[29] We utilized JAK1, JAK2 and JAK3 dependent Ba/F3 cell lines, where the JH1 domain of each JAK is fused with the oligomerization domain of TEL which results in constitutive tyrosine kinase activity and confers IL-3 independent proliferation.[26] In addition, we engineered a TYK2 Ba/F3 cell line whose proliferation is driven by constitutively activated TYK2 ($TYK2^{E957D}$).[30] As a further control, we also used a Ba/F3 cell line transformed by TEL- Abelson murine leukemia viral oncogene homolog (ABL). To enable a direct comparison with the commonly used JAK

Author Manuscript Author Manuscript Author Manuscript Author Manuscript

inhibitors we profiled reported compounds **1**–**5**,[4–5, 15b, 15g, 31] and **12**[32] against this panel of Ba/F3 cells. Compound **1** exhibited the most potent inhibition of JAK1 and JAK2 Ba/F3 cells, **2** exhibited most potent inhibition of JAK3 Ba/F3 cells and **3** exhibited most selective inhibition of JAK3 (Table S2). Overall the potency and selectivity of these inhibitors are consistent with their reported properties. Consistent with the biochemical assays, **9** selectively inhibited the proliferation of JAK3-dependent Ba/F3 cells (IC_{50} = 69 nM) relative to other JAK-dependent Ba/F3 cells, for which there was no antiproliferative effect at concentrations below 3.0 μM (Table 2). The general antiproliferative activity that appears at concentrations of approximately 3.0 μM could be due to inhibition of other kinases such as TTK (aka Mps1, IC_{50} = 49 nM) as inhibition of this kinase has been reported to decrease cancer cell viability.[33]

Co-crystal Structure of JAK3-Compound 9 Complex

To investigate the structural basis for achieving selectivity for JAK3 we solved the co-crystal structure of the JAK3 kinase domain in complex with **9** at a resolution of 2.9 Å (Figure 3). In this structure (PDB 4Z16), the anilinopyrimidine moiety of **9** makes the expected bidentate hinge hydrogen bonds with Leu905, and continuous electron density is observed between the acrylamide warhead and Cys909, indicative of covalent bond formation. The kinase exhibits an active conformation, with the DFG-motif in the inward position and both tyrosines 980 and 981 in the activation loop phosphorylated. The orientation and interactions of the anilinopyrimidine portion of the compound closely resembles the interactions observed in the $EGFR^{T790M}$-**8** co-crystal structure (PDB 3IKA)[21] (Figure S1). In addition to the hinge hydrogen bonds, the chlorine is directed towards the gatekeeper methionine (Met902 in the present structure) and the methoxy substituent extends toward the sidechain of Tyr904 in the hinge region. Interestingly, the “linker” segment that attaches the acrylamide adopts a distinctly different conformation as compared with the corresponding region of **8** in complex with $EGFR^{T790M}$. The phenyl group in the linker pivots down and is in van der Waals contact with Leu956 in the floor of the ATP-binding cleft. This orientation is likely enabled by the longer aminomethylene moiety in **9**, as compared with the ether linkage in compound **8**. In addition, the acrylamide amide is positioned to hydrogen bond with the carbonyl of Arg953, also in the floor of the binding pocket.

Structure-Activity Relationship (SAR) Studies Based on Compound 9

The syntheses of **9** was readily achieved with high-overall-yield in four steps starting from 2,4,5-trichloropyrimidine. The 4-chloride group was substituted with a 3-nitrobenzyl amine under basic conditions, followed by the substitution of the 2-chloride with a 2-methoxy-4-(4-methylpiperazin-1-yl)aniline under acidic conditions to give **11**. The nitro group of **11** was reduced using hydrogenation and the resulted aniline was acrylated to afford **9** (Scheme 1B). In order to elucidate the structural requirements to achieve potent and selective inhibition of JAK3 we prepared approximately 70 analogs. To approach this optimization in a systematic fashion, this chemotype was divided into three moieties: tail (R_1), arm (R_2) and core (R_3), and each of these moieties were varied sequentially. The 2,4-disubstited aniline tail moiety of **9** was replaced with different anilines, aliphatic amines or 4-aminopyrazoles;

Author Manuscript Author Manuscript Author Manuscript Author Manuscript

the 4-acrylamidobenzyl arm of **9** was substituted with functional groups at the double bond, phenyl ring or benzyl position; the pyrimidine core of **9** was modified at 5- or 6-position, or was replaced with a variety of bicyclic cores. All the analogs were profiled with the same JAK3 enzymatic assay and JAKs and ABL dependent Ba/F3 cell line assays. Additionally, the in vitro metabolic stability of some analogs was measured using mouse liver microsomes (MLM) to calculate half-lives ($T_{1/2}$).[34]

The first series of analogs focused on modification of the tail moiety (R_1) (Table 2). Substitutions at the 5-postion of the aniline (**14**, **15**) resulted in a dramatic loss of potency. In contrast, removing the 2-methoxy group (**16**) enhanced potency over 5-fold against JAK3, however, it also increased the cytotoxicity toward other transformed Ba/F3 cell lines. Substitutions at the 3-position did not mitigate the cytotoxicity (**17**–**19**), nor did introduction of a fluorine at the 2-position (**20**). Compound **21** with a 4-morpholinylaniline tail potently inhibited JAK3 despite not having the 2-methoxy substitution. Furthermore, **21** showed comparable cellular selectivity and MLM $T_{1/2}$ as **9** ($T_{1/2}$ of 4.7 min.). However, **21** only showed moderate selectivity in biochemical assays, with 10~20-fold higher IC_{50}s against JAK1, JAK2 or TTK (Table 1). Adding a 2- or 3-fluoro (**22**, **23**) did not improve the kinase selectivity of **21** and also did not improve the MLM stability. **24** which contains two fluorine substituents at the 2- and 5-positions showed good selectivity but decreased potency against JAK3. **25**, with 3,5-difluorine substitutions, exhibited improved potency compared to **24** with good selectivity in cells, even though it showed moderate selectivity in enzymatic assays. Based on **25** several analogs (**26**–**28**) were made and exhibited increased potency, but none of them were as selective as **25**. Aliphatic tails resulted in complete loss of potency (**29**–**31**). **32** with a 1-methyl-1*H*-pyrazol-3-amine tail showed increased potency, similar selectivity and MLM stability compared with **9**; it also showed a 300-fold selectivity window over TTK. Addition of a 4-methyl group to the pyrazole ring (**33**) enhanced the MLM stability but decreased the potency over 10-fold. The isoxazol-4-amine tail in **34** is disfavored in terms of both potency and stability. Modifications were then focused on the 1-methyl group of the pyrazole tail. Replacement of the 1-methyl with a 1-difluoromethyl (**35**) or a 1-difluoroethyl (**36**) maintained the potency and enhanced the MLM stability. However, bulky and hydrophobic substituents resulted in decreased MLM stability (**37**, **38**). **39** with a 2-substituted *N*-methylacetamide exhibited noticeably improved MLM stability ($T_{1/2}$ of 14.3 min) and favorable selectivity albeit with only moderate potency against JAK3. Nevertheless, other 2-substituted *N*-alkylacetamide groups (**40**–**42**) failed to improve the potency or stability. Several analogs elaborated with a 2-substituted ethyl group (**43**–**45**) showed good potency but decreased MLM stability. To our surprise, **45** with a 2-methoxyethyl exhibited an IC_{50} of 19 nM against JAK3 Ba/F3 cells, and over 390-fold selectivity over other Ba/F3 cell lines. **45** showed excellent selectivity with JAK3 IC_{50} of less than 0.5 nM in fixed end point enzymatic assay, and over 70-fold higher IC_{50} against JAK1 and over 100-fold higher IC_{50}s against JAK2, TYK2, TTK, BTK or ITK (Table 1, S1). **45** was profiled against a diverse panel of 468 kinases (DiscoveRX, KinomeScan[27]) at a concentration of 100 nM; the compound exhibited excellent overall kinase selectivity with selectivity scores, defined as the percentage of kinases with scores less than 5 (S(5))[27b], of 0.01 (Figure 4). The results suggested **45** inhibits JAK3 most potently, and aurora A (AURKA) was likely to be the only off-target which we confirmed to be inhibited by **45**

Author Manuscript Author Manuscript Author Manuscript Author Manuscript

with IC_{50} of 43 nM. **45** showed relatively poor MLM stability with $T_{1/2}$ of 3.3 min. Thus, several analogs with different 2-alkoxyethyl groups (**46**–**48**) were made to solve this problem. To our disappointment, all changes did not improve the MLM stability. Dimethyl substitution of the 2-methoxyethyl (**49**) is disfavored with respect to MLM stability as well as potency and selectivity. **50**, with a hydroxyl group in the tail, showed 3-fold longer MLM $T_{1/2}$ compared with **45**. Although **50** was not as selective as **45** in Ba/F3 cell lines, it was more potent than **9** with comparable selectivity in Ba/F3 cells. Further modification of **50** failed to improve the selectivity but led to decreased potency and MLM stability (**51**). In this series of analogs, **45** and **50** stood out with good selectivity or MLM stability, furthermore, we found **50** was actually one of the MLM metabolites of **45** (Figure S2).

After optimization of the tail moiety, the SAR of the arm (R_2) was investigated (Table 3). Replacing the acrylamide with a propionamide (**52**) resulted in over an 80-fold decrease of potency against JAK3. Installation of a methyl group at α-position of the acrylamide (**53**) resulted in significant loss of potency and a shorter MLM $T_{1/2}$. Polar substitutions at the β-position of the acrylamide (**54**–**56**) also resulted in loss of potency. Addition of a fluorine ortho to the acrylamide in the phenyl ring (**57**) also decrease the potency dramatically. Switching the acrylamide from *meta*- to *para*- on the phenyl ring decreased the potency considerably in combination with the aniline tail of **9** (**58**), but did not affect the potency when used in conjunction with other tails (**59**–**62**). This change did however decrease the selectivity in some cases (**59**, **62**). Analogs with a *para*-acrylamide generally showed comparable or diminished MLM stability. Finally, adding a methyl at the benzyl position (**63**, **64**) reduced both potency and selectivity. In summary, the modifications of R_2 failed to further improve our JAK3 inhibitors. Several reported inhibitors with similar acrylamide warheads (**6**, **7**, **8** and AZD9291[35] (**65**)) were also profiled and compared, none of them showed good inhibition against JAK3 Ba/F3 cells with IC_{50}s over 1.0 μM (Table S2).

Simultaneously we investigated the SAR of the core moiety (R_3) (Table 4). We found that a thioether linkage at the 4-postion (**66**, **67**) slightly increased the MLM stability but decreased the potency, and a tertiary amine linkage (-NMe-) decreased the potency even more dramatically (**68**). Next we investigated the effects of various substituents at the 5-position. We evaluated substituents that possessed electron withdrawing groups such as chlorine (**69**–**72**), electron donating groups (**73**–**75**) or simply a hydrogen atom (**76**). However, only **70** with a 5-bromo group showed good potency among these analogs. A 4,6-disubstituted pyrimidine core (**77**) also led to substantial loss of potency. Next we tried to cyclize the 4,5-substituents into a fused 5-membered or 6-membered ring (**78**–**82**), and found that only **78** with a pyrrolo[2,3-*d*]pyrimidine core showed good potency against JAK3, but with a slightly decreased MLM stability. **81** with a pyrimido[4,5-*d*]pyrimidinone core possessed a good IC_{50} against JAK3 in the biochemical assay, but mediocre potency in the TEL-JAK3-transformed Ba/F3 cells. In the end, modifications at the 6-position of the pyrimidine core (**83**, **84**) were fairly disfavored. These results suggested that 5-chlorine is the most suitable, and the secondary amine (-NH-) is a satisfactory linkage at 4-postion; some bicyclic cores did improve the inhibitor modestly, and modifications at 6-position are not tolerated.

Author Manuscript Author Manuscript Author Manuscript Author Manuscript

Validation of the Target-Engagement and the Covalent Binding

Based on the SAR results above, we selected **9**, **45** and **50** as our optimal JAK3 inhibitors, and investigated their inhibitory activity on JAK3-dependent signaling. As STAT5 has been reported as a direct substrate of TEL-JAK3 in Ba/F3 cells,[26] we examined the effect of our JAK3 inhibitors on STAT5 phosphorylation in this context. As we expected, STAT5 was constitutively phosphorylated in the cells treated with DMSO (Figure S3). Compound **2** at 300 nM almost fully inhibited the phosphorylation of STAT5 (p-STAT5), while **9** at 300 nM completely abolished p-STAT5, and so did **45** or **50** at 100 nM. These results are consistent with the IC_{50}s in JAK-transformed Ba/F3 proliferation assays. In order to confirm that **45** and **50** are bonafide covalent inhibitors in analogy to compound **9** we performed cellular 'wash-out' experiments. JAK3 Ba/F3 cells were treated with these four inhibitors at various concentrations for 3 h, the cells were washed extensively with PBS and then allowed to recover for 4 h. Western blots of the cellular lysates revealed that **9**, **45** or **50** were capable of sustained inhibition of p-STAT5 after the washout, whereas the reversible inhibitor **2** was not (Figure 5A). To monitor the degree of JAK3 'target engagement', a biotinylated version of **45** (**85**) was designed with a biotin tethered via a flexible PEG linker at the tip of **45**'s tail moiety (Figure 5C). We confirmed that **85** maintained similar biochemical potency and selectivity for JAK3 (Table 1). **85** showed selective but weak potency against JAK3 Ba/F3 cells with an IC_{50} of 1.3 μM (Table S2) presumably due to poor membrane permeability. We demonstrated that streptavidin mediated pulldown of **85** in cell lysates allowed for efficient recovery of JAK3 as assessed by western blotting. Consistent with the wash-out results, **85** strongly labeled JAK3 when cells were treated with the reversible inhibitor **2** but not when cells were treated with acrylamide modified inhibitors **9**, **45** or **50** (Figure 5B). Compounds **9**, **45** and **50** were further demonstrated to be covalent inhibitors using electrospray ionization mass spectrometry, where incubation of recombinant JAK3 kinase domain with inhibitor resulted in addition of the expected molecular weight (Figure 6). Subsequent protease digestion and LC/MS^2 experiments identified a single modified peptide LVMEYLPSGC*LR (C*, cysteine labeled by **9**, **45** or **50**, JAK3 residues 900–911) and localized the site of modification to Cys909 (Figure S4), in agreement with the JAK3/**9** co-crystal structure. Cumulatively these results provide strong evidence that **9**, **45** and **50** are all irreversible, covalent inhibitors and that Cys909 of JAK3 is the only labeled site.

Validation in Cells with Endogenous JAK3

Compounds **9**, **45** and **50** were further evaluated for their ability to inhibit JAK3 kinase activity in a variety of other cell types. We evaluated the ability of **9**, **45** or **50** to inhibit signaling following stimulation of primary murine bone marrow derived macrophage (BMDMs) with a panel of 4 different cytokines based on their requirement for different cytokines (Figure 7). Among these cytokines, only signaling via IL-4, whose receptor binds JAK1 and JAK3,[36] is dependent on JAK3. In contrast, granulocyte-macrophage colony-stimulating factor (GM-CSF), which signals via JAK2, and IL-10 and interferon beta (IFNβ), which signal via JAK1 and TYK2, are JAK3 independent.[37] **9**, **45** or **50** completely inhibited IL-4 induced p-STAT6 at a concentration of 500 nM and only partially inhibited IFNβ-induced p-STAT1 at a concentration of 5.0 μM. None of our inhibitors detectably reduced the p-STAT5 level stimulated by GM-CSF or p-STAT3 induced by IL-10 at a

Author Manuscript Author Manuscript Author Manuscript Author Manuscript

concentration of 5.0 μM. While demonstrating excellent selectivity in Ba/F3 cellular assays, these inhibitors showed decreased but still decent selectivity in primary cells. The washout experiments with **45** or **50** in BMDMs cells exhibited consistent results as in TEL-JAK3 Ba/F3 cells, and suggested that the inhibitory effect lasted for at least 24 h after the washout (Figure S5). In a similar way, **9**, **45** and **50** exhibited consistent potency and selectivity for JAK3 in leukemia cancer cell lines: T-ALL1 and OCL-AML5 (Figure 8). In T-ALL1 cells, IL-2 induced STAT5 phosphorylation was completely inhibited by **9** at a concentration of 1.0 μM or by **45** or **50** at a concentration of 100 nM (Figure 8A). However, in OCL-AML5 cells the GM-CSF induced STAT5 phosphorylation was maintained in the presence of the inhibitors up to a concentration of 10 μM (Figure 8B). In contrast, previously reported pan-JAK inhibitors **1** and **2** could abolish p-STAT5 in both stimulated cell lines at 1.0 μM. Based on these results compounds **9**, **45** and **50** are capable of efficiently inhibiting JAK3 and specifically blocking the JAK3-dependent signaling pathway in human cells at sub-micromolar concentrations.

Mouse Pharmacokinetic Properties and In Vivo Studies

We evaluated the pharmacokinetic properties of **9** in mice following intravenous and oral delivery. Compound **9** demonstrated reasonable pharmacokinetic properties, with moderate $T_{1/2}$ of 1.4 h, area under the curve (AUC) value of 795 ng*hr/mL following a 10 mg/Kg oral dose and good oral bioavailability of 66% (Table 5). This suggests that **9** may be a suitable probe for future murine efficacy studies. We evaluated the ability of compound **9** to alter immune cell numbers in genetically engineered models (GEM) of lung adenocarcinoma in mice. Immune cell numbers in mice harboring tumors driven by $Kras^{G12D};Lkb1^{L/L}$–[38] were assessed in tumor-associated (lung) as well as general immune cell populations (spleen) upon treatment with compound **9**. After oral administration with **9** (75 mpk, QD) for 8 days, the numbers of B or T lymphocytes in the tumor-bearing lungs and spleens of treated mice was not affected, however, the number of NK cells was reduced (Figure S6). Similarly, the number of tumor-associated macrophages and neutrophils in the lung of treated mice were not affected. During the short duration of this study, we did not detect any effect on the tumor growth.

Discussion

Building on our covalent T790M EGFR inhibitor **8** we designed and synthesized new analogs aiming to target the analogous cysteine residue in JAK3. Among those analogs compound **9** was identified as a potent and selective JAK3 inhibitor compared with current reversible JAK inhibitors. We determined a 2.9 Å co-crystal structure of JAK3 with **9**, which revealed that **9** covalently binds to Cys909 of JAK3 as expected. With **9** as a lead, we designed and synthesized dozens of analogs to intensively study the SAR with regard to each moiety of this scaffold. These analogs were tested in enzymatic assays for their potency against JAK3 and profiled against a panel of transformed Ba/F3 cell lines, for their potency and selectivity in a cellular context. Based on these studies we discovered that a 2-methoxy group in the aniline tail of **9** is disfavored by JAK3 presumably due to a disfavored interaction with the bulky side chain of Tyr904 located at the GK+2 position. Hydrophobic or less polar tails are better for selectivity for JAK3 presumably because they have weaker

Author Manuscript Author Manuscript Author Manuscript Author Manuscript

non-covalent affinity for the kinase thereby allowing covalent bond formation to be a more important contributor to the potency. The acrylamidobenzyl arm moiety of **9** is significant for the potency against JAK3 and sensitive to changes, its specific length and flexibility are critical to enable the inhibitors to efficiently form a covalent bond with Cys909 of JAK3. The H-bond between the acrylamide of **9** and the carbonyl of Arg953 fixed the conformation of the acrylamide and left no space to accommodate substituents. The chlorine atom in the pyrimidine core is responsible for both potency and selectivity with its interaction with Met902 of JAK3. Modifications at the 6-position of the pyrimidine core were fairly disfavored as they collided with the carbonyl of Glu903 3.3Å away. Some of these analogs were also evaluated for their MLM stability, the results indicated that more lipophilic analogs with aliphatic non-polar substituents tend to have a shorter half-life, maybe resulting from their enhanced binding with phospholipid in microsomes.[39]

Among these analogs **9**, **45** and **50** stood out with overall favorable potency, selectivity and MLM stability. They all exhibited efficient and selective inhibition of JAK-dependent signaling within different contexts. So far **45** is our most selective JAK3 inhibitor with at least 70-fold selectivity over other JAKs in biochemically assays, at least 390-fold selectivity in JAK-transformed Ba/F3 cells, and decent selectivity in primary cells. In addition to the evidence provided by JAK3-**9** co-crystal structure, all three inhibitors were demonstrated to covalently modify Cys909 of JAK3 based upon wash-out and pull-down experiments and mass spectrometry. We developed a biotinylated probe **85** which was demonstrated to be a useful reagent for establishing “target-engagement” in cellular assays. We also found that a short-term treatment with high dose of compound **9** in mice with lung tumors resulted in a decrease in the number of NK cells suggesting that the compounds are active *in vivo*. Further investigations will be required to elucidate the basis for this phenomena and to assess the activity of covalent JAK3 inhibitors in relevant disease models.

In conclusion, the covalent JAK3 inhibitors **9**, **45**, **50**, and the biotinylated probe **85** provide a set of useful tools to pharmacologically interrogate JAK3-dependent biology. Compound **45** is a highly potent and selective biochemical and cellular inhibitor of JAK3 and is an ideal reagent for cell biological studies. Compound **9** combines favorable target profile with good pharmacokinetic properties and is ready to be used in future animal studies. Finally, the structure-activity relationships with respect to JAK3 combined with the co-crystal structure will serve as an excellent foundation for future JAK3 inhibitor development efforts.

Experimental Section

Chemistry

Unless otherwise noted, reagents and solvents were obtained from commercial suppliers and were used without further purification. ^{1}H NMR spectra were recorded on 600 MHz (Varian AS600), and chemical shifts are reported in parts per million (ppm, δ) downfield from tetramethylsilane (TMS). Coupling constants (*J*) are reported in Hz. Spin multiplicities are described as s (singlet), br (broad singlet), d (doublet), t (triplet), q (quartet), and m (multiplet). Mass spectra were obtained on a Waters Micromass ZQ instrument. Preparative HPLC was performed on a Waters Sunfire C18 column (19 × 50 mm, 5μM) using a gradient of 15–95% methanol in water containing 0.05% trifluoroacetic acid (TFA) over 22 min (28

Author Manuscript Author Manuscript Author Manuscript Author Manuscript

min run time) at a flow rate of 20 mL/min. Purities of assayed compounds were in all cases greater than 95%, as determined by reverse-phase HPLC analysis.

2,5-Dichloro-*N*-(3-nitrobenzyl)pyrimidin-4-amine (10)

2,4,5-Trichloropyrimidine (112 μL, 1.0 mmol), (3-nitrophenyl)methanamine hydrochloride salt (227 mg, 1.2 mmol), and *N*,*N*-diisopropylethylamine (DIEA, 530 μL, 3.0 mmol) were combined in dioxane (5 mL) and stirred overnight. The mixture was then diluted with ethyl acetate and washed with water and brine, dried over Na_2SO_4, filtered and concentrated. The crude product was purified by column chromatography (hexane:ethyl acetate = 1:1) to yield 270 mg (80%) of **10** as a white solid. ^{1}H NMR (600 MHz, $CDCl_3$) δ 8.21 (s, 1H), 8.18 (d, *J* = 8.4 Hz, 1H), 8.10 (s, 1H), 7.71 (d, *J* = 7.8 Hz, 1H), 7.56 (dd, *J* = 7.8, 7.8 Hz, 1H), 5.94 (br, 1H), 4.84 (d, *J* = 6.0 Hz, 1H). MS (ESI) m/z 299 $(M+H)^+$.

5-Chloro-N^2-(2-methoxy-4-(4-methylpiperazin-1-yl)phenyl)-N^4-(3-nitrobenzyl)pyrimidine-2,4-diamine (11)

To **10** (150 mg, 0.5 mmol) and 2-methoxy-4-(4-methylpiperazin-1-yl)aniline (166 mg, 0.75 mmol) in *sec*-butanol (5 mL) was added trifluoroacetic acid (57 μL, 0.75 mmol) and the mixture was stirred overnight at 100 °C. The mixture was then concentrated, neutralized with ammonia in methanol and purified by column chromatography (dichloromethane:methanol = 10:1) to yield 184 mg (76%) of **11** as a pale-yellow solid. ^{1}H NMR (600 MHz, CD_3OD) δ 8.23 (s, 1H), 8.09 (d, *J* = 8.4 Hz, 1H), 7.84 (s, 1H), 7.70 (d, *J* = 7.8 Hz, 1H), 7.65 (d, *J* = 9.0 Hz, 1H), 7.54 (dd, *J* = 7.8, 7.8 Hz, 1H), 6.60 (d, *J* = 3.0 Hz, 1H), 6.36 (dd, *J* = 9.0, 3.0 Hz, 1H), 4.75 (s, 1H), 3.83 (s, 3H), 3.15 (m, 4H), 2.64 (m, 4H), 2.36 (s, 3H). MS (ESI) *m/z* 484 $(M+H)^+$.

N-(3-(((5-chloro-2-((2-methoxy-4-(4-methylpiperazin-1-yl)phenyl)amino)pyrimidin-4-yl)amino)methyl)phenyl)acrylamide (9)

To **11** (97 mg, 0.2 mmol) in MeOH (20 mL) was added 1 mL Raney nickel suspension in MeOH. The reaction mixture was stirred for 3 h under 1 atm of hydrogen. The mixture was then filtered with Celite, and the filtrate was concentrated and dried under vacuum to give a crude product as a white solid. To the obtained white solid in DMF (2 mL) was added DIEA (53 μL, 0.3 mmol), the stirred mixture was then cooled to −60 °C, and acryloyl chloride (17.8 μL, 0.22 mmol) was added dropwise. The reaction mixture was stirred at −60 °C for 10 min, allowed to recover to RT (room temperature) gradually in 30 min, and purified by reverse phase HPLC to give 88 mg (TFA salt, 71% for 2 steps) of **9** as a white solid. ^{1}H NMR (600 MHz, DMSO-d_6) δ 10.07 (s, 1H), 7.82 (s, 1H), 7.73 (m, 1H), 7.59 (s, 1H), 7.52 (d, *J* = 8.4 Hz, 1H), 7.47 (d, *J* = 7.8 Hz, 1H), 7.29 (s, 1H), 7.18 (dd, *J* = 7.8, 7.8 Hz, 1H), 6.90 (d, *J* = 7.2 Hz, 1H), 6.48 (s, 1H), 6.44 (dd, *J* = 16.8, 10.2 Hz, 1H), 6.31 (d, *J* = 8.4 Hz, 1H), 6.25 (d, *J* = 16.8 Hz, 1H), 5.75 (d, *J* = 10.2 Hz, 1H), 4.56 (d, *J* = 6.0 Hz, 2H), 3.78 (s, 3H), 3.04 (m, 4H), 3.01 (m, 4H), 2.22 (s, 3H). MS (ESI) *m/z* 508 $(M+H)^+$.

Compound **14**–**64**, **66**–**85** were synthesized with same procedures as **9**, **3** and **8** were synthesized as reported.[19, 31] Compound **1**, **2**, **6**, **7**, **12**, **13** and **65** were from Selleckchem, **4** was from Santa Cruz, and **5** was from Millipore.

Author Manuscript Author Manuscript Author Manuscript Author Manuscript

Enzymatic assays

The enzymatic activities against JAK1, JAK2, JAK3, TYK2, FLT3, BLK, TXK, BTK, ITK and AURKA were tested in Z'-Lyte assays with ATP concentrations of Km for each kinases, the activities against TTK were tested in LanthaScreen binding assays. All the protocols are available from Life Technologies.[40]

Protein expression and purification

Human JAK3 kinase domain (residues 811–1124) was expressed and purified as described previously[41] except that JAK3 was co-expressed with human c-SRC (residues 86–536) to achieve more consistent phosphorylation of JAK3.

Crystallization and structure determination

Crystals of JAK3 in complex with **9** were prepared using the hanging drop vapor diffusion method; JAK3 at a concentration of 5 mg/mL was incubated for 30 min with 500 μM compound **9**, then added to an equal volume of well solution (0.1 M bis-tris pH 6.5, 0.2 M ammonium sulfate, 16% PEG 3350, 5 mM TCEP) and equilibrated over well solution at 4 °C. Crystals were looped into cryoprotectant solution (0.1 M bis-tris pH 6.5, 0.2 M ammonium sulfate, 20 % PEG 3350, 15% glycerol, 5 mM TCEP) for 30–60 sec, then flash-frozen in liquid nitrogen. X-ray diffraction data were collected at APS beamline 24-ID-E (NE-CAT), processed with XDS,[42] and scaled with Scala.[43] The structure was solved by molecular replacement with Phaser[44] using the JAK3 kinase domain as a search model (PDB 1YVJ).[41] Manual refitting of the crystallographic model was performed with Coot[45] and refinement was performed with Phenix[46] and BUSTER.[47] Topology and parameter files for compound **9** were generated with PRODRG.[48]

Mass spectrometry

JAK3 protein (5 μg) was labeled with a 10-fold excess of inhibitor or DMSO for 30 minutes at 4 °C. After labeling, proteins were desalted using 0.5 mL Zeba spin desalting columns (Thermo Fisher Scientific). Analysis of intact protein was performed essentially as described.[49] Briefly, ~5 μg protein was injected onto a self-packed reversed-phase column (500 μm inner diameter, 5 cm of POROS 50R2 resin). After washing to remove salts, protein was eluted with an HPLC gradient (0%–100% B in 1 min, A = 0.2 M acetic acid in water, B = 0.2 M acetic acid in acetonitrile, flow rate = 10 μL/min) into a linear ion trap mass spectrometer (LTQ, Thermo Fisher Scientific, San Jose, CA). Data were acquired in profile mode scanning m/z 300–2000. Mass spectra were deconvoluted using MagTran software (version 1.03b2).[50] Sites of covalent modification were identified using a "bottom-up" strategy. Desalted proteins were reduced with tris(2-carboxyethyl)phosphine (10 mM, 10 min room temperature), alkylated with iodoacetamide (20 mM, 30 min room temperature in dark), and digested with trypsin for 4 h at 37 °C. Digests were analyzed by nanoLC-ESI-MS as described with modifications.[51] Peptides were loaded onto a self-packed pre-column (4 cm POROS10R2), resolved on an analytical column (30 μm I.D., packed with 12 cm C18) and eluted into the mass spectrometer (LTQ Orbitrap XL, Thermo Fisher Scientific) using an HPLC gradient (Waters NanoAcquity, Milford, MA; 0%–35% B in 60 min, A = 0.2 M acetic acid in water, B = 0.2 M acetic acid in acetonitrile, flow rate = ~30 nL/min). The

Author Manuscript Author Manuscript Author Manuscript Author Manuscript

instrument was operated in data dependent mode such that the top 10 most abundant precursors were subjected to MS/MS (electron multiplier detection, relative collision energy 35%, q = 0.25). Raw data files were converted to .mgf using in-house software[52] and searched using Mascot 2.2.1 against a forward-reverse human refseq database. Search parameters specified variable oxidation of methionine, variable inhibitor modification (**9**, **45**, or **50**) of cysteine, and fixed carbamidomethylation of cysteine (i.e. cysteines are considered carbamidomethylated or inhibitor labeled). To confirm labeling sites, internally calibrated HCD spectra (image current detection, resolution at *m/z* 200 = 15,000, relative collision energy 35%) were acquired using an Orbitrap Fusion mass spectrometer (Thermo Fisher Scientific). For these experiments, LC parameters were similar to those described above, except that the analytical column was packed with 50 cm of C18 and peptides were eluted with a gradient of 0–35% B in 90 min.

Mouse liver microsomal stability

The MLM assays were previously reported and are commercially available from Scripps Florida.[34]

Ba/F3 cell viability assays

Ba/F3 derivatives expressing various oncogenic fusion kinases, TEL-JAK1, TEL-JAK2, TEL-JAK3 and TEL-ABL were described previously.[26] Ba/F3 cells transformed by $TYK2^{E957D}$ were generated as previously described.[30] These cells were maintained in RPMI-1640 medium (GIBCO) supplemented with 10% fetal bovine serum (FBS) (Sigma-Aldrich) and penicillin/streptomycin (Invitrogen). For cell viability assays, the cells were plated at a density of 10,000 cells per well in a 96-well white plate and incubated with DMSO or increasing concentrations of drugs. At 72 h after the initiation of treatment, the relative cell viability was determined using the Cell Titer Glo assay (Promega) and reported as a percentage of the DMSO control. Concentration values for 50% inhibition (IC_{50}) of cell viability were determined with GraphPad Prism software.

Immunoblotting analysis and washout experiment

Ba/F3 cells transformed by TEL-JAK3 were incubated with JAK3 inhibitors or DMSO for 3 h. Then whole-cell lysates were prepared in RIPA buffer (Cell Signaling) with FOCUS™, ProteaseArrest™ (G-Biosciences) and Phosphatase Inhibitor Cocktail Set II (EMD Millipore). Western blotting analyses were conducted after separation by SDS-PAGE electrophoresis and transfer to nitrocellulose membranes. Immunoblotting was performed with each of specific antibodies to STAT5, phospho-STAT5 (Tyr694), α-tubulin (Cell Signaling Tech) and JAK3 (Santa Cruz, #sc-513). For washout experiment, cells were incubated with JAK3 inhibitors or DMSO for 3 h, washed with PBS three times, maintained in RPMI-1640 medium with 10% of FBS for 4 h, and then harvested and the resulting lysates were analyzed. Primary bone marrow derived macrophages (BMDMs) were prepared as described.[53] Cells were maintained on bacterial grade DMEM supplemented with 10% heat-inactivated fetal bovine serum, 2 mM L-glutamine, 100 U/ml of penicillin G, 100 μg/ml of streptomycin, 0.25 μg/ml of amphotericin (Invitrogen), and 5 ng/ml of macrophage colony-stimulating factor (M-CSF; PreProTech) for 7 days. Cells were then replated onto

Author Manuscript Author Manuscript Author Manuscript Author Manuscript

tissue culture grade plastic and used the following day. Following stimulation cells were lsyed into SDS sample buffer and run on 10% polyacrylamide gels according to standard techniques. Proteins were transferred onto nitrocellulose membranes and blotted with antibodies against total ERK1/2, p-Y641 STAT6, p-Y701 STAT1, pY701 STAT3 or pY694 STAT5 (all from Cell Signaling Tech). The experiments in cancer cell lines were done with similar procedures.

Streptavidin pulldown experiment

Ba/F3 cells transformed by TEL-JAK3 were incubated with JAK3 inhibitors or DMSO for 3 h, and then lysed with Pierce IP lysis buffer (Thermo Scientific) with Halt™ protease inhibitor cocktail (Thermo Scientific). The lysates were treated with **85** (5 μM) at 4 °C overnight, and then further incubated at room temperature for 3 h. The solution was mixed with Streptavidin beads (25 μL, Sigma) and incubated with rotation at 4 °C for 2 h. The beads were washed five times using the lysis buffer with 4 M urea (1 mL), and then boiled in the presence of Lammli sample buffer with 2-mercaptoethanol. The eluted proteins were immunoblotted with each of specific antibodies.

In Vivo Pharmacokinetic Studies

Male Swiss albino mice were dosed via tail vein (intravenous, 0.1% *v/v* Tween 80, 0.5% *w/v* NaCMC in water at a dose of 10 mg/kg) or via oral gavage (suspensions in 5% NMP, 5% solutol HS in normal saline intravenously via tail vein at a dose of 2 mg/kg). Blood samples were collected at 0.08, 0.25, 0.5, 1, 2, 4, 8 and 24 h (i.v.) and at Predose, 0.25, 0.5, 1, 2, 4, 6, 8 and 24 h (p.o.). Plasma samples were separated by centrifugation of whole blood and stored below −70°C until bioanalysis. All samples were processed for analysis by protein precipitation using acetonitrile and analyzed with fit-for-purpose LC/MS/MS method (LLOQ, 1.06 ng/mL). Pharmacokinetic parameters were calculated using the non-compartmental analysis tool of WinNonlin Enterprise software (version 6.3).

Mouse treatment studies

Kras^{G12D}*;Lkb1*$^{L/L}$ mice were intrathoracically injected with adenovirus expressing Cre recombinase (2.5×10^7 PFU/10 μl) at 6 weeks of age to initiate tumor formation.[38b] All experimental mice were maintained on a mixed genetic background (C57Bl/6, Balb-c, and S129). MR imaging and tumor quantification were performed as described previously.[38b] Compound **9** and vehicle controls were given per os once daily at a 75 mpk dose.

Total mouse lung cell and tumor infiltrating immune cell characterization was performed as previously described.[54] Splenocytes were isolated similarly without collagenase treatment. The antibodies used for immune analysis are listed in supplementary methods. Acquisition of eight color samples was performed on a BD Canto II cytometer equipped with Diva software and analyzed using Flowjo. All *in vivo* experiments performed in the PK studies and this study were approved by the Animal Care and Use Committee of the Dana-Farber Cancer Institute.

Author Manuscript Author Manuscript Author Manuscript Author Manuscript

Supplementary Material

Refer to Web version on PubMed Central for supplementary material.

Acknowledgments

We thank Dr. Cai-Hong Yun for his valuable help with creating topology and parameter files for the refinement of the JAK3-**9** co-crystal structure. The TEL-JAK1, TEL-JAK2, TEL-JAK3 and TEL-ABL plasmids used in this studies were generously provided by Dr. Richard Moriggl. G.S.H.-S. was supported by the Deutsche Forschungsgemeinschaft (HE 6897/1-1). We thank Dr. Ying Li for data analysis and Dr. Sara Buhrlage for the proof-reading.

References

1. (a) Darnell JE Jr, Kerr IM, Stark GR. Jak-STAT pathways and transcriptional activation in response to IFNs and other extracellular signaling proteins. Science. 1994; 264(5164):1415–1421. [PubMed: 8197455] (b) Stark GR, Darnell JE Jr. The JAK-STAT pathway at twenty. Immunity. 2012; 36(4): 503–514. [PubMed: 22520844]
2. (a) O'Shea JJ, Gadina M, Schreiber RD. Cytokine signaling in 2002: new surprises in the Jak/Stat pathway. Cell. 2002; 109(Suppl):S121–131. [PubMed: 11983158] (b) Ghoreschi K, Laurence A, O'Shea JJ. Janus kinases in immune cell signaling. Immunological reviews. 2009; 228(1):273–287. [PubMed: 19290934]
3. (a) Johnston JA, Bacon CM, Riedy MC, O'Shea JJ. Signaling by IL-2 and related cytokines: JAKs, STATs, and relationship to immunodeficiency. Journal of leukocyte biology. 1996; 60(4):441–452. [PubMed: 8864127] (b) Boudny V, Kovarik J. JAK/STAT signaling pathways and cancer. Janus kinases/signal transducers and activators of transcription. Neoplasma. 2002; 49(6):349–355. [PubMed: 12584581] (c) Baker SJ, Rane SG, Reddy EP. Hematopoietic cytokine receptor signaling. Oncogene. 2007; 26(47):6724–6737. [PubMed: 17934481] (d) Villarino AV, Kanno Y, Ferdinand JR, O'Shea JJ. Mechanisms of Jak/STAT signaling in immunity and disease. J Immunol. 2015; 194(1):21–27. [PubMed: 25527793] (e) O'Shea JJ, Schwartz DM, Villarino AV, Gadina M, McInnes IB, Laurence A. The JAK-STAT pathway: impact on human disease and therapeutic intervention. Annual review of medicine. 2015; 66:311–328.
4. Quintas-Cardama A, Vaddi K, Liu P, Manshouri T, Li J, Scherle PA, Caulder E, Wen X, Li Y, Waeltz P, Rupar M, Burn T, Lo Y, Kelley J, Covington M, Shepard S, Rodgers JD, Haley P, Kantarjian H, Fridman JS, Verstovsek S. Preclinical characterization of the selective JAK1/2 inhibitor INCB018424: therapeutic implications for the treatment of myeloproliferative neoplasms. Blood. 2010; 115(15):3109–3117. [PubMed: 20130243]
5. Flanagan ME, Blumenkopf TA, Brissette WH, Brown MF, Casavant JM, Shang-Poa C, Doty JL, Elliott EA, Fisher MB, Hines M, Kent C, Kudlacz EM, Lillie BM, Magnuson KS, McCurdy SP, Munchhof MJ, Perry BD, Sawyer PS, Strelevitz TJ, Subramanyam C, Sun J, Whipple DA, Changelian PS. Discovery of CP-690,550: a potent and selective Janus kinase (JAK) inhibitor for the treatment of autoimmune diseases and organ transplant rejection. Journal of medicinal chemistry. 2010; 53(24):8468–8484. [PubMed: 21105711]
6. (a) Tam CS, Verstovsek S. Investigational Janus kinase inhibitors. Expert opinion on investigational drugs. 2013; 22(6):687–699. [PubMed: 23432430] (b) Clark JD, Flanagan ME, Telliez JB. Discovery and development of Janus kinase (JAK) inhibitors for inflammatory diseases. Journal of medicinal chemistry. 2014; 57(12):5023–5038. [PubMed: 24417533] (c) Rosenthal A, Mesa RA. Janus kinase inhibitors for the treatment of myeloproliferative neoplasms. Expert opinion on pharmacotherapy. 2014; 15(9):1265–1276. [PubMed: 24766055] (d) Mascarenhas JO, Cross NC, Mesa RA. The future of JAK inhibition in myelofibrosis and beyond. Blood reviews. 2014; 28(5): 189–196. [PubMed: 25043171] (e) Geyer HL, Mesa RA. Therapy for myeloproliferative neoplasms: when, which agent, and how? Blood. 2014; 124(24):3529–3537. [PubMed: 25472969]
7. (a) Menet CJ, Rompaey LV, Geney R. Advances in the discovery of selective JAK inhibitors. Progress in medicinal chemistry. 2013; 52:153–223. [PubMed: 23384668] (b) Dymock BW, Yang EG, Chu-Farseeva Y, Yao L. Selective JAK inhibitors. Future medicinal chemistry. 2014; 6(12): 1439–1471. [PubMed: 25329199] (c) Norman P. Selective JAK inhibitors in development for

Author Manuscript Author Manuscript Author Manuscript Author Manuscript

rheumatoid arthritis. Expert opinion on investigational drugs. 2014; 23(8):1067–1077. [PubMed: 24818516]

8. Rochman Y, Spolski R, Leonard WJ. New insights into the regulation of T cells by gamma(c) family cytokines. Nature reviews Immunology. 2009; 9(7):480–490.
9. Wang X, Lupardus P, Laporte SL, Garcia KC. Structural biology of shared cytokine receptors. Annual review of immunology. 2009; 27:29–60.
10. Casanova JL, Holland SM, Notarangelo LD. Inborn errors of human JAKs and STATs. Immunity. 2012; 36(4):515–528. [PubMed: 22520845]
11. Cornejo MG, Boggon TJ, Mercher T. JAK3: a two-faced player in hematological disorders. The international journal of biochemistry & cell biology. 2009; 41(12):2376–2379. [PubMed: 19747563]
12. Bains T, Heinrich MC, Loriaux MM, Beadling C, Nelson D, Warrick A, Neff TL, Tyner JW, Dunlap J, Corless CL, Fan G. Newly described activating JAK3 mutations in T-cell acute lymphoblastic leukemia. Leukemia. 2012; 26(9):2144–2146. [PubMed: 22425895]
13. (a) Walters DK, Mercher T, Gu TL, O'Hare T, Tyner JW, Loriaux M, Goss VL, Lee KA, Eide CA, Wong MJ, Stoffregen EP, McGreevey L, Nardone J, Moore SA, Crispino J, Boggon TJ, Heinrich MC, Deininger MW, Polakiewicz RD, Gilliland DG, Druker BJ. Activating alleles of JAK3 in acute megakaryoblastic leukemia. Cancer cell. 2006; 10(1):65–75. [PubMed: 16843266] (b) Koo GC, Tan SY, Tang T, Poon SL, Allen GE, Tan L, Chong SC, Ong WS, Tay K, Tao M, Quek R, Loong S, Yeoh KW, Yap SP, Lee KA, Lim LC, Tan D, Goh C, Cutcutache I, Yu W, Ng CC, Rajasegaran V, Heng HL, Gan A, Ong CK, Rozen S, Tan P, Teh BT, Lim ST. Janus kinase 3-activating mutations identified in natural killer/T-cell lymphoma. Cancer discovery. 2012; 2(7): 591–597. [PubMed: 22705984]
14. Van Allen EM, Golay HG, Liu Y, Koyama S, Wong K, Taylor-Weiner A, Giannakis M, Harden M, Rojas-Rudilla V, Chevalier A, Thai T, Lydon C, Mach S, Avila AG, Wong JA, Rabin AR, Helmkamp J, Sholl L, Carter SL, Oxnard G, Janne P, Getz G, Lindeman N, Hammerman PS, Garraway LA, Hodi FS, Rodig SJ, Dranoff G, Wong KK, Barbie DA. Long-term Benefit of PD-L1 Blockade in Lung Cancer Associated with JAK3 Activation. Cancer immunology research. 2015
15. (a) Narla RK, Liu XP, Myers DE, Uckun FM. 4-(3′-Bromo-4′hydroxylphenyl)-amino-6,7-dimethoxyquinazoline: a novel quinazoline derivative with potent cytotoxic activity against human glioblastoma cells. Clinical cancer research : an official journal of the American Association for Cancer Research. 1998; 4(6):1405–1414. [PubMed: 9626456] (b) Chen JJ, Thakur KD, Clark MP, Laughlin SK, George KM, Bookland RG, Davis JR, Cabrera EJ, Easwaran V, De B, George Zhang Y. Development of pyrimidine-based inhibitors of Janus tyrosine kinase 3. Bioorganic & medicinal chemistry letters. 2006; 16(21):5633–5638. [PubMed: 16934457] (c) Soth M, Hermann JC, Yee C, Alam M, Barnett JW, Berry P, Browner MF, Frank K, Frauchiger S, Harris S, He Y, Hekmat-Nejad M, Hendricks T, Henningsen R, Hilgenkamp R, Ho H, Hoffman A, Hsu PY, Hu DQ, Itano A, Jaime-Figueroa S, Jahangir A, Jin S, Kuglstatter A, Kutach AK, Liao C, Lynch S, Menke J, Niu L, Patel V, Railkar A, Roy D, Shao A, Shaw D, Steiner S, Sun Y, Tan SL, Wang S, Vu MD. 3-Amido pyrrolopyrazine JAK kinase inhibitors: development of a JAK3 vs JAK1 selective inhibitor and evaluation in cellular and in vivo models. Journal of medicinal chemistry. 2013; 56(1):345–356. [PubMed: 23214979] (d) de Vicente J, Lemoine R, Bartlett M, Hermann JC, Hekmat-Nejad M, Henningsen R, Jin S, Kuglstatter A, Li H, Lovey AJ, Menke J, Niu L, Patel V, Petersen A, Setti L, Shao A, Tivitmahaisoon P, Vu MD, Soth M. Scaffold hopping towards potent and selective JAK3 inhibitors: discovery of novel C-5 substituted pyrrolopyrazines. Bioorganic & medicinal chemistry letters. 2014; 24(21):4969–4975. [PubMed: 25262541] (e) Gehringer M, Pfaffenrot E, Bauer S, Laufer SA. Design and synthesis of tricyclic JAK3 inhibitors with picomolar affinities as novel molecular probes. ChemMedChem. 2014; 9(2):277–281. [PubMed: 24403205] (f) Jaime-Figueroa S, De Vicente J, Hermann J, Jahangir A, Jin S, Kuglstatter A, Lynch SM, Menke J, Niu L, Patel V, Shao A, Soth M, Vu MD, Yee C. Discovery of a series of novel 5H-pyrrolo[2,3-b]pyrazine-2-phenyl ethers, as potent JAK3 kinase inhibitors. Bioorganic & medicinal chemistry letters. 2013; 23(9):2522–2526. [PubMed: 23541670] (g) Thoma G, Nuninger F, Falchetto R, Hermes E, Tavares GA, Vangrevelinghe E, Zerwes HG. Identification of a potent Janus kinase 3 inhibitor with high selectivity within the Janus kinase family. Journal of medicinal chemistry. 2011; 54(1):284–288. [PubMed: 21155605] (h) McDonnell ME, Bian H, Wrobel J,

Author Manuscript Author Manuscript Author Manuscript Author Manuscript

Smith GR, Liang S, Ma H, Reitz AB. Anilino-monoindolylmaleimides as potent and selective JAK3 inhibitors. Bioorganic & medicinal chemistry letters. 2014; 24(4):1116–1121. [PubMed: 24461299] (i) Ross JA, Spadaro M, Rosado DC, Cavallo F, Kirken RA, Pericle F. Inhibition of JAK3 with a novel, selective and orally active small molecule induces therapeutic response in T-cell malignancies. Leukemia. 2014; 28(4):941–944. [PubMed: 24153015]

16. (a) Changelian PS, Flanagan ME, Ball DJ, Kent CR, Magnuson KS, Martin WH, Rizzuti BJ, Sawyer PS, Perry BD, Brissette WH, McCurdy SP, Kudlacz EM, Conklyn MJ, Elliott EA, Koslov ER, Fisher MB, Strelevitz TJ, Yoon K, Whipple DA, Sun J, Munchhof MJ, Doty JL, Casavant JM, Blumenkopf TA, Hines M, Brown MF, Lillie BM, Subramanyam C, Shang-Poa C, Milici AJ, Beckius GE, Moyer JD, Su C, Woodworth TG, Gaweco AS, Beals CR, Littman BH, Fisher DA, Smith JF, Zagouras P, Magna HA, Saltarelli MJ, Johnson KS, Nelms LF, Des Etages SG, Hayes LS, Kawabata TT, Finco-Kent D, Baker DL, Larson M, Si MS, Paniagua R, Higgins J, Holm B, Reitz B, Zhou YJ, Morris RE, O'Shea JJ, Borie DC. Prevention of organ allograft rejection by a specific Janus kinase 3 inhibitor. Science. 2003; 302(5646):875–878. [PubMed: 14593182] (b) Pattison MJ, Mackenzie KF, Arthur JS. Inhibition of JAKs in macrophages increases lipopolysaccharide-induced cytokine production by blocking IL-10-mediated feedback. J Immunol. 2012; 189(6):2784–2792. [PubMed: 22904308]
17. (a) Liao W, Spolski R, Li P, Du N, West EE, Ren M, Mitra S, Leonard WJ. Opposing actions of IL-2 and IL-21 on Th9 differentiation correlate with their differential regulation of BCL6 expression. Proceedings of the National Academy of Sciences of the United States of America. 2014; 111(9):3508–3513. [PubMed: 24550509] (b) Bouchekioua A, Scourzic L, de Wever O, Zhang Y, Cervera P, Aline-Fardin A, Mercher T, Gaulard P, Nyga R, Jeziorowska D, Douay L, Vainchenker W, Louache F, Gespach C, Solary E, Coppo P. JAK3 deregulation by activating mutations confers invasive growth advantage in extranodal nasal-type natural killer cell lymphoma. Leukemia. 2014; 28(2):338–348. [PubMed: 23689514]
18. Liu Q, Sabnis Y, Zhao Z, Zhang T, Buhrlage SJ, Jones LH, Gray NS. Developing irreversible inhibitors of the protein kinase cysteinome. Chemistry & biology. 2013; 20(2):146–159. [PubMed: 23438744]
19. Li D, Ambrogio L, Shimamura T, Kubo S, Takahashi M, Chirieac LR, Padera RF, Shapiro GI, Baum A, Himmelsbach F, Rettig WJ, Meyerson M, Solca F, Greulich H, Wong KK. BIBW2992, an irreversible EGFR/HER2 inhibitor highly effective in preclinical lung cancer models. Oncogene. 2008; 27(34):4702–4711. [PubMed: 18408761]
20. Brown JR. Ibrutinib (PCI-32765), the first BTK (Bruton's tyrosine kinase) inhibitor in clinical trials. Current hematologic malignancy reports. 2013; 8(1):1–6. [PubMed: 23296407]
21. Zhou W, Ercan D, Chen L, Yun CH, Li D, Capelletti M, Cortot AB, Chirieac L, Iacob RE, Padera R, Engen JR, Wong KK, Eck MJ, Gray NS, Janne PA. Novel mutant-selective EGFR kinase inhibitors against EGFR T790M. Nature. 2009; 462(7276):1070–1074. [PubMed: 20033049]
22. Flanagan ME, Abramite JA, Anderson DP, Aulabaugh A, Dahal UP, Gilbert AM, Li C, Montgomery J, Oppenheimer SR, Ryder T, Schuff BP, Uccello DP, Walker GS, Wu Y, Brown MF, Chen JM, Hayward MM, Noe MC, Obach RS, Philippe L, Shanmugasundaram V, Shapiro MJ, Starr J, Stroh J, Che Y. Chemical and computational methods for the characterization of covalent reactive groups for the prospective design of irreversible inhibitors. Journal of medicinal chemistry. 2014; 57(23):10072–10079. [PubMed: 25375838]
23. Zambaldo C, Sadhu KK, Karthikeyan G, Barluenga S, Daguer JP, Winssinger N. Selective affinity-based probe for oncogenic kinases suitable for live cell imaging. Chemical Science. 2013; 4(5):2088–2092.
24. London N, Miller RM, Krishnan S, Uchida K, Irwin JJ, Eidam O, Gibold L, Cimermancic P, Bonnet R, Shoichet BK, Taunton J. Covalent docking of large libraries for the discovery of chemical probes. Nature chemical biology. 2014; 10(12):1066–1072. [PubMed: 25344815]
25. Goedken ER, Argiriadi MA, Banach DL, Fiamengo BA, Foley SE, Frank KE, George JS, Harris CM, Hobson AD, Ihle DC, Marcotte D, Merta PJ, Michalak ME, Murdock SE, Tomlinson MJ, Voss JW. Tricyclic Covalent Inhibitors Selectively Target Jak3 through an Active Site Thiol. The Journal of biological chemistry. 2015; 290(8):4573–4589. [PubMed: 25552479]

Author Manuscript Author Manuscript Author Manuscript Author Manuscript

26. Lacronique V, Boureux A, Monni R, Dumon S, Mauchauffe M, Mayeux P, Gouilleux F, Berger R, Gisselbrecht S, Ghysdael J, Bernard OA. Transforming properties of chimeric TEL-JAK proteins in Ba/F3 cells. Blood. 2000; 95(6):2076–2083. [PubMed: 10706877]
27. (a) Goldstein DM, Gray NS, Zarrinkar PP. High-throughput kinase profiling as a platform for drug discovery. Nature reviews Drug discovery. 2008; 7(5):391–397. [PubMed: 18404149] (b) Miduturu CV, Deng X, Kwiatkowski N, Yang W, Brault L, Filippakopoulos P, Chung E, Yang Q, Schwaller J, Knapp S, King RW, Lee JD, Herrgard S, Zarrinkar P, Gray NS. High-throughput kinase profiling: a more efficient approach toward the discovery of new kinase inhibitors. Chemistry & biology. 2011; 18(7):868–879. [PubMed: 21802008]
28. Lebakken CS, Riddle SM, Singh U, Frazee WJ, Eliason HC, Gao Y, Reichling LJ, Marks BD, Vogel KW. Development and applications of a broad-coverage, TR-FRET-based kinase binding assay platform. Journal of biomolecular screening. 2009; 14(8):924–935. [PubMed: 19564447]
29. Warmuth M, Kim S, Gu XJ, Xia G, Adrian F. Ba/F3 cells and their use in kinase drug discovery. Current opinion in oncology. 2007; 19(1):55–60. [PubMed: 17133113]
30. Sanda T, Tyner JW, Gutierrez A, Ngo VN, Glover J, Chang BH, Yost A, Ma W, Fleischman AG, Zhou W, Yang Y, Kleppe M, Ahn Y, Tatarek J, Kelliher MA, Neuberg DS, Levine RL, Moriggl R, Muller M, Gray NS, Jamieson CH, Weng AP, Staudt LM, Druker BJ, Look AT. TYK2-STAT1-BCL2 pathway dependence in T-cell acute lymphoblastic leukemia. Cancer discovery. 2013; 3(5):564–577. [PubMed: 23471820]
31. Fleischmann RM, Damjanov NS, Kivitz AJ, Legedza A, Hoock T, Kinnman N. A Randomized, Double-Blind, Placebo-Controlled, Twelve-Week, Dose-Ranging Study of Decernotinib, an Oral Selective JAK-3 Inhibitor, as Monotherapy in Patients With Active Rheumatoid Arthritis. Arthritis Rheumatol. 2015; 67(2):334–343. [PubMed: 25385260]
32. Pardanani A, Lasho T, Smith G, Burns CJ, Fantino E, Tefferi A. CYT387, a selective JAK1/JAK2 inhibitor: in vitro assessment of kinase selectivity and preclinical studies using cell lines and primary cells from polycythemia vera patients. Leukemia. 2009; 23(8):1441–1445. [PubMed: 19295546]
33. Kwiatkowski N, Jelluma N, Filippakopoulos P, Soundararajan M, Manak MS, Kwon M, Choi HG, Sim T, Deveraux QL, Rottmann S, Pellman D, Shah JV, Kops GJ, Knapp S, Gray NS. Small-molecule kinase inhibitors provide insight into Mps1 cell cycle function. Nature chemical biology. 2010; 6(5):359–368. [PubMed: 20383151]
34. Li X, He Y, Ruiz CH, Koenig M, Cameron MD, Vojkovsky T. Characterization of dasatinib and its structural analogs as CYP3A4 mechanism-based inactivators and the proposed bioactivation pathways. Drug metabolism and disposition: the biological fate of chemicals. 2009; 37(6):1242–1250. [PubMed: 19282395]
35. Cross DA, Ashton SE, Ghiorghiu S, Eberlein C, Nebhan CA, Spitzler PJ, Orme JP, Finlay MR, Ward RA, Mellor MJ, Hughes G, Rahi A, Jacobs VN, Red Brewer M, Ichihara E, Sun J, Jin H, Ballard P, Al-Kadhimi K, Rowlinson R, Klinowska T, Richmond GH, Cantarini M, Kim DW, Ranson MR, Pao W. AZD9291, an irreversible EGFR TKI, overcomes T790M-mediated resistance to EGFR inhibitors in lung cancer. Cancer discovery. 2014; 4(9):1046–1061. [PubMed: 24893891]
36. Cortes JR, Perez GM, Rivas MD, Zamorano J. Kaempferol inhibits IL-4-induced STAT6 activation by specifically targeting JAK3. J Immunol. 2007; 179(6):3881–3887. [PubMed: 17785825]
37. O'Sullivan LA, Liongue C, Lewis RS, Stephenson SE, Ward AC. Cytokine receptor signaling through the Jak-Stat-Socs pathway in disease. Molecular immunology. 2007; 44(10):2497–2506. [PubMed: 17208301]
38. (a) Ji H, Ramsey MR, Hayes DN, Fan C, McNamara K, Kozlowski P, Torrice C, Wu MC, Shimamura T, Perera SA, Liang MC, Cai D, Naumov GN, Bao L, Contreras CM, Li D, Chen L, Krishnamurthy J, Koivunen J, Chirieac LR, Padera RF, Bronson RT, Lindeman NI, Christiani DC, Lin X, Shapiro GI, Janne PA, Johnson BE, Meyerson M, Kwiatkowski DJ, Castrillon DH, Bardeesy N, Sharpless NE, Wong KK. LKB1 modulates lung cancer differentiation and metastasis. Nature. 2007; 448(7155):807–810. [PubMed: 17676035] (b) Herter-Sprie GS, Korideck H, Christensen CL, Herter JM, Rhee K, Berbeco RI, Bennett DG, Akbay EA, Kozono D,

Author Manuscript Author Manuscript Author Manuscript Author Manuscript

Mak RH, Mike Makrigiorgos G, Kimmelman AC, Wong KK. Image-guided radiotherapy platform using single nodule conditional lung cancer mouse models. Nature communications. 2014; 5:5870.

39. Eling TE, DiAugustine RP. A role for phospholipids in the binding and metabolism of drugs by hepatic microsomes. Use of the fluorescent hydrophobic probe 1-anilinonaphthalene-8-sulphonate. The Biochemical journal. 1971; 123(4):539–549. [PubMed: 5126906]

40. Z'-Lyte assays: http://www.lifetechnologies.com/content/dam/LifeTech/migration/files/drug-discovery/pdfs.par.60256.file.dat/20130430%20ssbk%20customer%20protocol%20and%20assay%20conditions.pdf; TTK assay: http://tools.lifetechnologies.com/content/sfs/manuals/TTK_LanthaScreen_Binding.pdf

41. Boggon TJ, Li Y, Manley PW, Eck MJ. Crystal structure of the Jak3 kinase domain in complex with a staurosporine analog. Blood. 2005; 106(3):996–1002. [PubMed: 15831699]

42. Kabsch W. Xds. Acta crystallographica Section D, Biological crystallography. 2010; 66(Pt 2):125–132. [PubMed: 20124692]

43. (a) Evans P. Scaling and assessment of data quality. Acta crystallographica Section D, Biological crystallography. 2006; 62(Pt 1):72–82. [PubMed: 16369096] (b) Winn MD, Ballard CC, Cowtan KD, Dodson EJ, Emsley P, Evans PR, Keegan RM, Krissinel EB, Leslie AG, McCoy A, McNicholas SJ, Murshudov GN, Pannu NS, Potterton EA, Powell HR, Read RJ, Vagin A, Wilson KS. Overview of the CCP4 suite and current developments. Acta crystallographica Section D, Biological crystallography. 2011; 67(Pt 4):235–242. [PubMed: 21460441]

44. McCoy AJ, Grosse-Kunstleve RW, Adams PD, Winn MD, Storoni LC, Read RJ. Phaser crystallographic software. Journal of applied crystallography. 2007; 40(Pt 4):658–674. [PubMed: 19461840]

45. Emsley P, Lohkamp B, Scott WG, Cowtan K. Features and development of Coot. Acta crystallographica Section D, Biological crystallography. 2010; 66(Pt 4):486–501. [PubMed: 20383002]

46. Adams PD, Afonine PV, Bunkoczi G, Chen VB, Davis IW, Echols N, Headd JJ, Hung LW, Kapral GJ, Grosse-Kunstleve RW, McCoy AJ, Moriarty NW, Oeffner R, Read RJ, Richardson DC, Richardson JS, Terwilliger TC, Zwart PH. PHENIX: a comprehensive Python-based system for macromolecular structure solution. Acta crystallographica Section D, Biological crystallography. 2010; 66(Pt 2):213–221. [PubMed: 20124702]

47. Bricogne, G.; Blanc, E.; Brandl, M.; Flensburg, C.; Keller, P.; Paciorek, W.; Roversi, P.; Sharff, A.; Smart, OS.; Vonrhein, C.; Womack, TO. BUSTER version 2.10.2. Cambridge, United Kingdom: Global Phasing Ltd; 2011.

48. Schuttelkopf AW, van Aalten DM. PRODRG: a tool for high-throughput crystallography of protein-ligand complexes. Acta crystallographica Section D, Biological crystallography. 2004; 60(Pt 8):1355–1363. [PubMed: 15272157]

49. Zhang T, Inesta-Vaquera F, Niepel M, Zhang J, Ficarro SB, Machleidt T, Xie T, Marto JA, Kim N, Sim T, Laughlin JD, Park H, LoGrasso PV, Patricelli M, Nomanbhoy TK, Sorger PK, Alessi DR, Gray NS. Discovery of potent and selective covalent inhibitors of JNK. Chemistry & biology. 2012; 19(1):140–154. [PubMed: 22284361]

50. Zhang Z, Marshall AG. A universal algorithm for fast and automated charge state deconvolution of electrospray mass-to-charge ratio spectra. Journal of the American Society for Mass Spectrometry. 1998; 9(3):225–233. [PubMed: 9879360]

51. Ficarro SB, Zhang Y, Lu Y, Moghimi AR, Askenazi M, Hyatt E, Smith ED, Boyer L, Schlaeger TM, Luckey CJ, Marto JA. Improved electrospray ionization efficiency compensates for diminished chromatographic resolution and enables proteomics analysis of tyrosine signaling in embryonic stem cells. Analytical chemistry. 2009; 81(9):3440–3447. [PubMed: 19331382]

52. Askenazi M, Parikh JR, Marto JA. mzAPI: a new strategy for efficiently sharing mass spectrometry data. Nature methods. 2009; 6(4):240–241. [PubMed: 19333238]

53. McGuire VA, Gray A, Monk CE, Santos SG, Lee K, Aubareda A, Crowe J, Ronkina N, Schwermann J, Batty IH, Leslie NR, Dean JL, O'Keefe SJ, Boothby M, Gaestel M, Arthur JS. Cross talk between the Akt and p38alpha pathways in macrophages downstream of Toll-like receptor signaling. Molecular and cellular biology. 2013; 33(21):4152–4165. [PubMed: 23979601]

Author Manuscript Author Manuscript Author Manuscript Author Manuscript

54. Akbay EA, Koyama S, Carretero J, Altabef A, Tchaicha JH, Christensen CL, Mikse OR, Cherniack AD, Beauchamp EM, Pugh TJ, Wilkerson MD, Fecci PE, Butaney M, Reibel JB, Soucheray M, Cohoon TJ, Janne PA, Meyerson M, Hayes DN, Shapiro GI, Shimamura T, Sholl LM, Rodig SJ, Freeman GJ, Hammerman PS, Dranoff G, Wong KK. Activation of the PD-1 pathway contributes to immune escape in EGFR-driven lung tumors. Cancer discovery. 2013; 3(12):1355–1363. [PubMed: 24078774]

Author Manuscript Author Manuscript Author Manuscript Author Manuscript

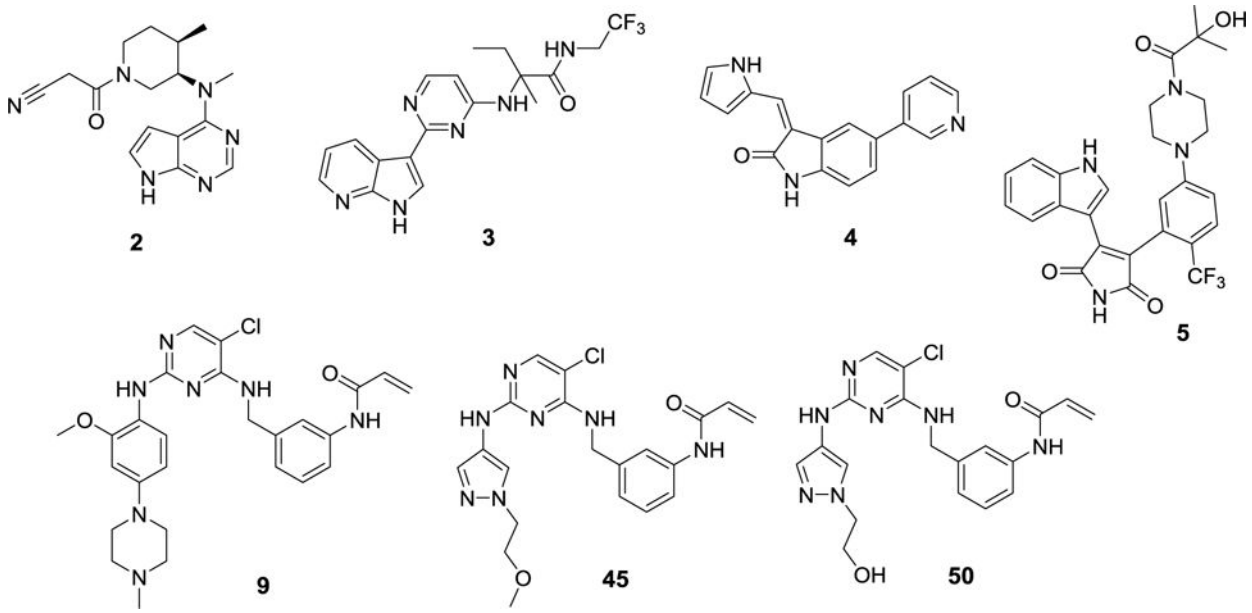

Figure 1.

Structures of exemplary JAK3 inhibitors **(2–5)** and lead compounds (**9, 45** and **50**) in this work.

Author Manuscript Author Manuscript Author Manuscript Author Manuscript

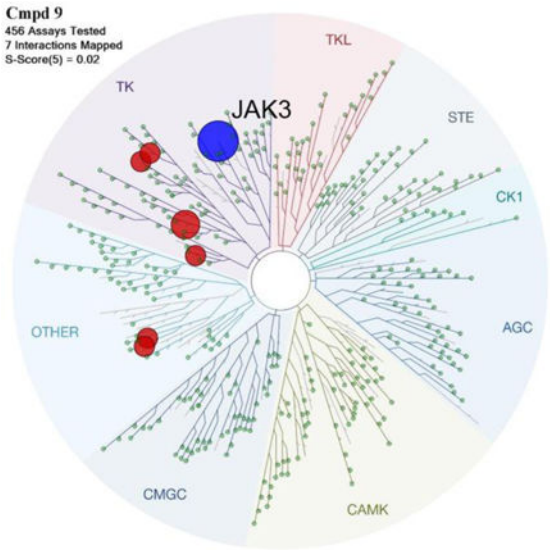

Kinases	Score (%)
JAK3	0
FLT3	0.6
TTK	1.4
BLK	1.6
TXK	3.4
FAK	4
CAMKK2	4.2
GAK	5.4
LTK	5.9
ERBB4	6
SGK	6.8
ARK5	9.6
PDGFRB	9.6
TNK1	9.9

Figure 2.

KinomeScan kinase selectivity profiles for Compound **9**. Compound **9** were profiled at a concentration of 1 μM against a diverse panel of more than 456 kinases and mutants. Scores for primary screen hits were reported as a percent of the DMSO control (% control). The lower the Kd is likely to be, such that scores of zero represent strong hits. Scores are related to the probability of being a hit but are not strictly an affinity measurement.

Author Manuscript Author Manuscript Author Manuscript Author Manuscript

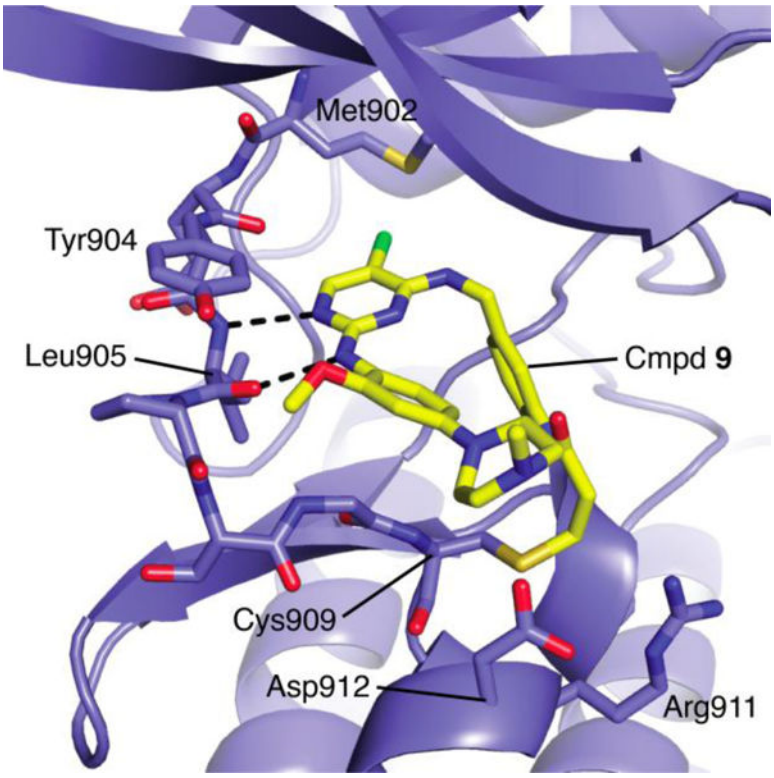

Figure 3.

X-ray co-crystal structure of JAK3-**9** (PDB 4Z16). Compound **9** (yellow sticks) covalently binds to Cys909 at the GK+7 position of JAK3 (blue ribbons). The hydrogen bonds between the anilinopyrimidine moiety of **9** and Leu905 in the JAK3 hinge region are indicated.

Author Manuscript Author Manuscript Author Manuscript Author Manuscript

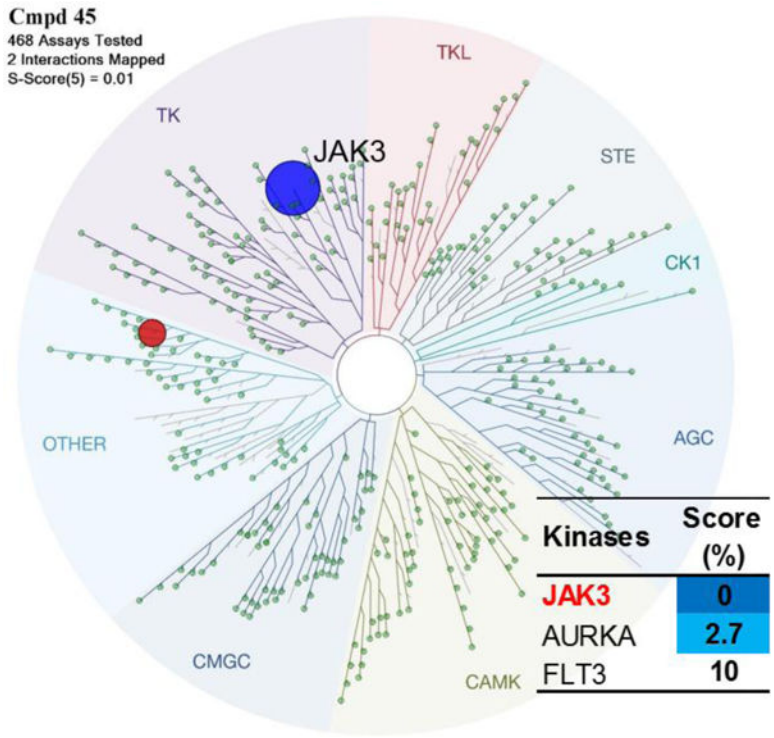

Figure 4.

KinomeScan kinase selectivity profiles for Compound **45**. Compound **45** were profiled at a concentration of 100 nM against a diverse panel of more than 468 kinases and mutants. Scores for primary screen hits are reported as a percent of the DMSO control (% control). The lower the Kd is likely to be, such that scores of zero represent strong hits. Scores are related to the probability of a hit but are not strictly an affinity measurement.

Author Manuscript Author Manuscript Author Manuscript Author Manuscript

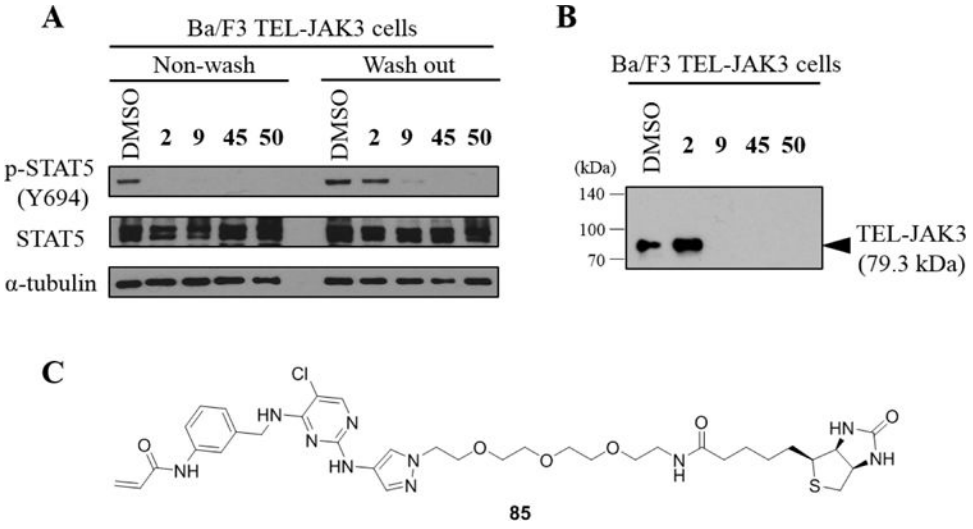

Figure 5.

Compounds **9**, **45**, and **50** are covalent, irreversible JAK3 inhibitors. TEL-JAK3 Ba/F3 cells were treated with **2**, **9** (1.0 μM), **45** or **50** (300 nM) for 3 h, washed extensively with PBS, allowed to recover for 4 h, then lysed and subjected to western blot for phospho-STAT5 and total STAT5 (A). TEL-JAK3 Ba/F3 cells were treated **2**, **9** (1.0 μM), **45** or **50** (300 nM) for 3 h, and the resulting cell lysates were treated with **85** (C) (1.0 μM, 1 h), followed by pull-down with streptavidin beads and immunoblotting with anti-JAK3 antibody (B).

Author Manuscript Author Manuscript Author Manuscript Author Manuscript

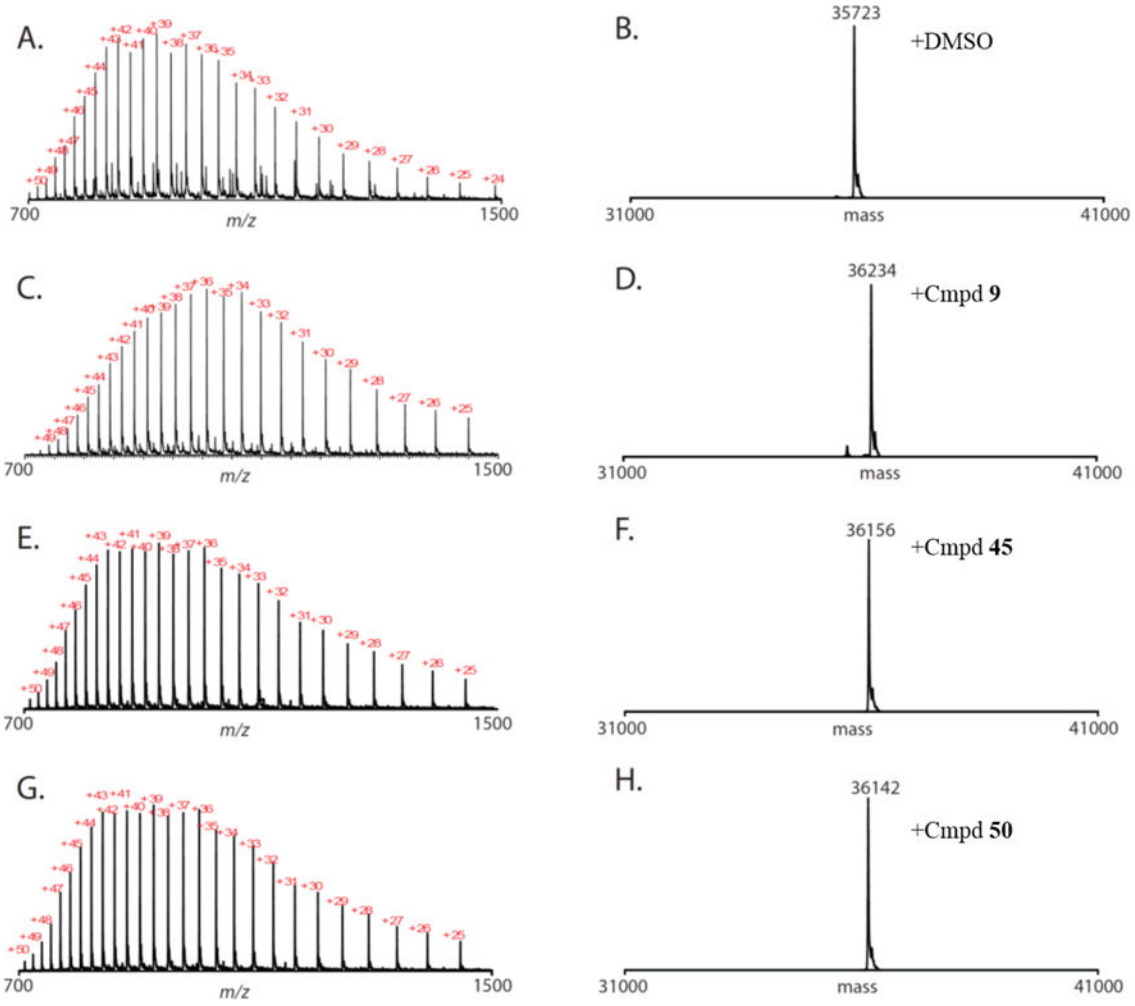

Figure 6.

Compound **9**, **45**, or **50** react quantitatively with JAK3. Raw (A, C, E, G) and deconvoluted (B, D, F, H) mass-spectra obtained for JAK3 after treatment with DMSO (A, B), **9** (C, D), **45** (E, F), or **50** (G, H).

Author Manuscript Author Manuscript Author Manuscript Author Manuscript

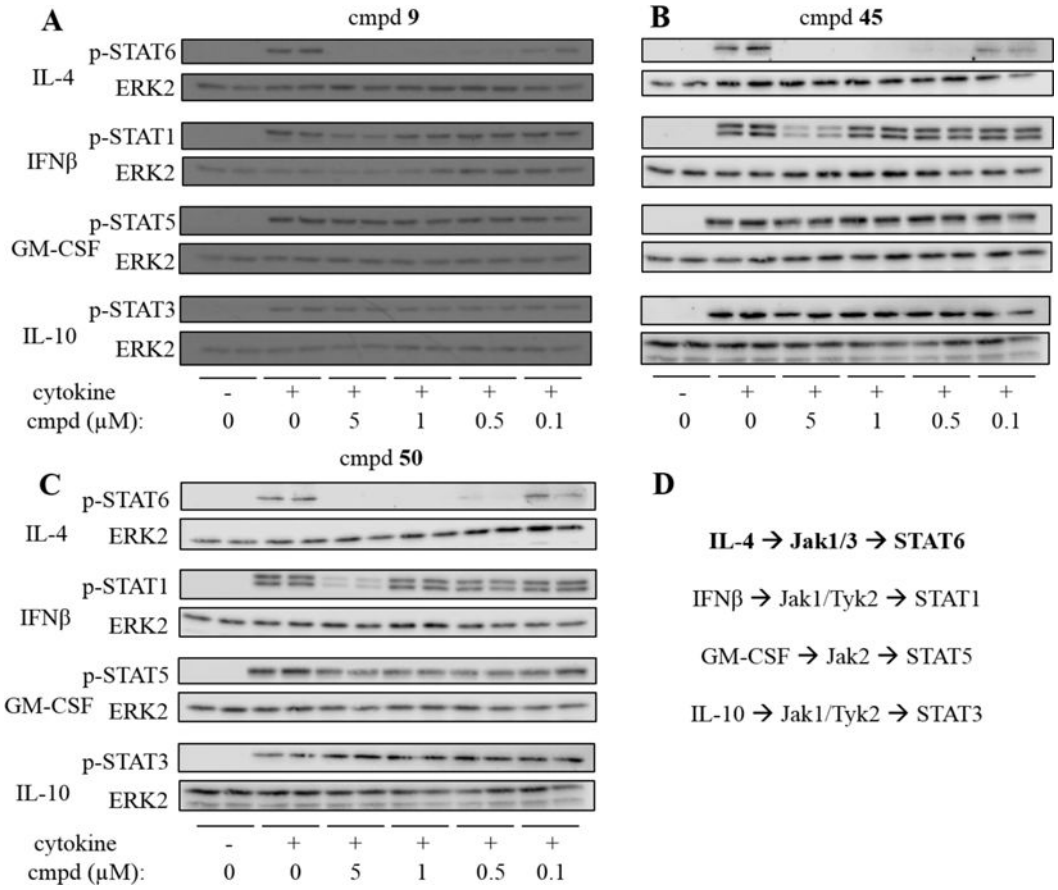

Figure 7.

Compound **9**, **45** or **50** potently and selectively inhibited JAK3-dependent signaling in BMDMs cells. BMDMs cells were pre-incubated with the indicated concentrations of **9** (A), **45** (B) or **50** (C) for 3 h. Cells were then stimulated with the indicated cytokines (IL-4 at 10 ng/mL, IFNβ at 500 U/mL, GM-CSF at 10 ng/mL, and IL-10 at 100 ng/mL) for 30 min then lysed. The levels of tyrosine phosphorylation on the appropriate STAT protein were determined by immunoblotting. Levels of total ERK1/2 were also examined to show equal loading. The signaling cascades were described in D.

Author Manuscript Author Manuscript Author Manuscript Author Manuscript

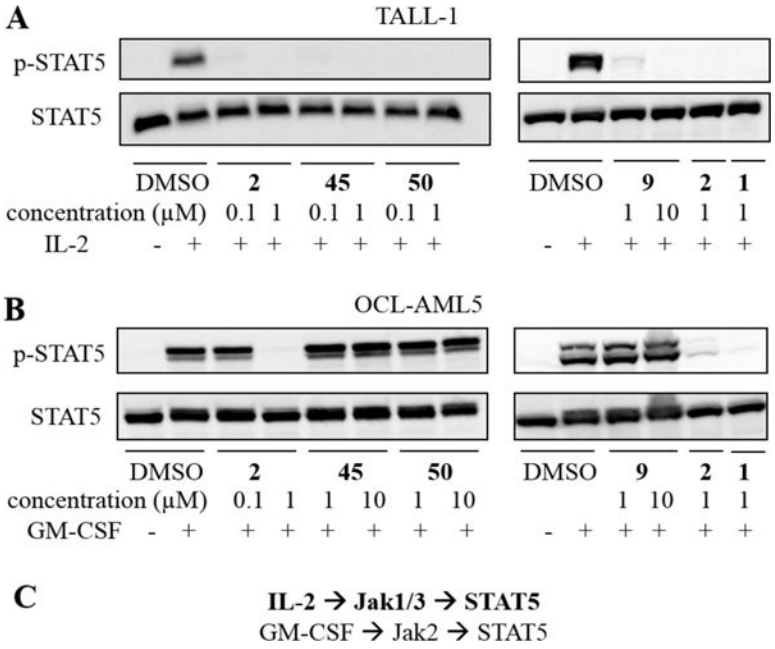

Figure 8.

Compound **9**, **45** and **50** potently and selectively inhibited JAK3-dependent p-STAT5 in TALL-1 cells whereas pan-JAK inhibitors **1** and **2** also potently inhibited JAK2-dependent p-STAT5 in OCL-AML5 cells. TALL-1 (A) or OCL-AML5 (B) cells were pre-incubated with the indicated concentrations of indicated inhibitors for 3 h. Cells were then stimulated with 10 ng/mL of IL-2 (A) or 5 ng of GM-CSF (B) for 30 min then lysed. The p-STAT5 levels were determined by immunoblotting. Levels of total STAT5 were also examined to show equal loading. The signaling cascades were described in C.

Author Manuscript Author Manuscript Author Manuscript Author Manuscript

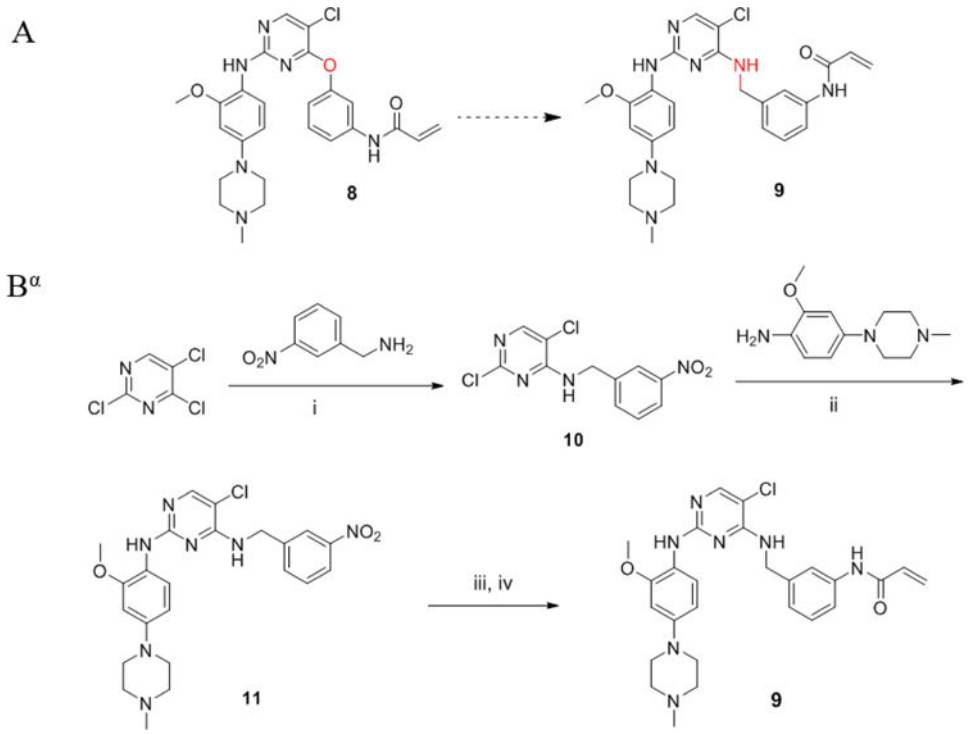

Scheme 1.

[α] i) DIEA, 1,4-dioxane, RT; ii) TFA, 2-BuOH, 100 °C; iii) Raney nickel, H_2, MeOH; iv) acryloyl chloride, sat. $NaHCO_3$, THF, 0 °C~RT.

Author Manuscript Author Manuscript Author Manuscript Author Manuscript

Table 1

Enzymatic IC_{50}s of key compounds [a]

	IC_{50}s (nM)				
Cmpd ID	**JAK1**	**JAK2**	**JAK3**	**TYK2**	**TTK**
9	896	1050	4.8	>10000	49
21	24.4	17.6	1.3		28.6
25	495	351	20		355
32	49	107	0.6		180
45	35	51	<0.5	407	212
50	11	32	<0.5	140	143
85	743	421	2.3	3120	

[a] IC_{50}s against JAK-family kinases were obtained with Z'-Lyte activity assays while IC_{50}s against TTK were obtained with LanthaScreen binding assays.

Author Manuscript Author Manuscript Author Manuscript Author Manuscript

Table 2

SAR of R_1

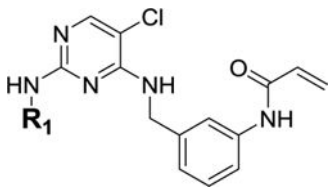

ID	R_1	JAK3 IC_{50} (nM)[a]	Ba/F3 cellular IC_{50}s (nM)[b]					MLM $T_{1/2}$ (min)[c]
			TEL-JAK1	TEL-JAK2	TEL-JAK3	TYK2 (E957D)	TEL-ABL	
9	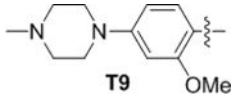 **T9**	4.8	3124±116	3194±619	69±13	2266±490	3047±116	4.7
14	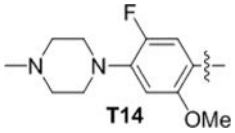 **T14**	46	3871	6175	1305	3756	5257	
15	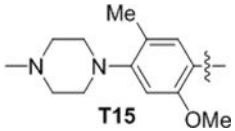 **T15**	170						
16	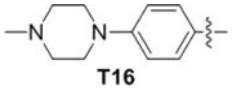 **T16**	1.2	513	1013	11	1320	2077	
17	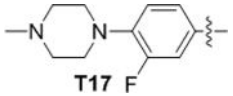 **T17**	0.9	821	993	15	599	1558	

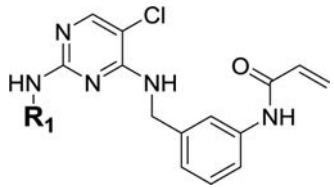

ID	R_1	JAK3 IC_{50} (nM)[a]	Ba/F3 cellular IC_{50}s (nM)[b]					MLM $T_{1/2}$ (min)[c]
			TEL-JAK1	TEL-JAK2	TEL-JAK3	TYK2 (E957D)	TEL-ABL	
18	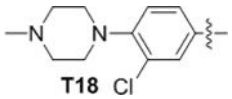	2.0	378	692	20	874	1932	
19	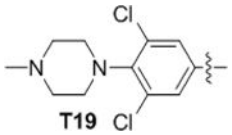	20	1059	2685	75	992	3470	
20	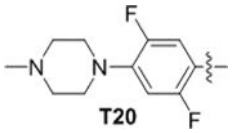	4.6	3182	5981	125	1318	2824	
21	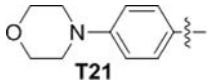	1.3	1857±581	3704±410	7±0.1	2353±201	13705±194	5.2
22	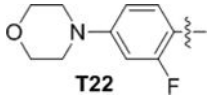	1.4	3287	2910	29	1542	4494	3
23	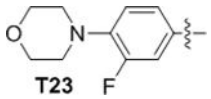	0.9	5195±3001	9087±4895	11±3.3	6613±2650	22410±4752	3

Author Manuscript Author Manuscript Author Manuscript Author Manuscript

Author Manuscript Author Manuscript Author Manuscript Author Manuscript

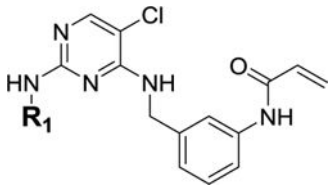

ID	R_1	JAK3 IC_{50} (nM)[a]	Ba/F3 cellular IC_{50}s (nM)[b]					MLM $T_{1/2}$ (min)[c]
			TEL-JAK1	TEL-JAK2	TEL-JAK3	TYK2 (E957D)	TEL-ABL	
24	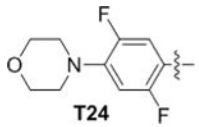 T24	5.2	>5E4	>5E4	478	>5E4	>5E4	
25	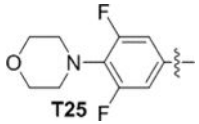 T25	20	>5E4	>5E4	99	>5E4	>5E4	
26	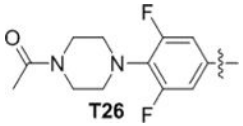 T26	3.6	2004	3290	23	4666	8769	3.4
27	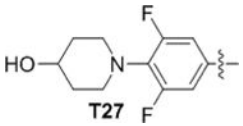 T27	7.4	2484	4321	35	4702	2326	
28	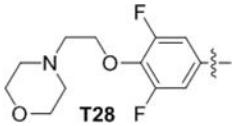 T28	6.2	2346	2916	54	4171	5477	
29	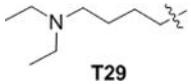 T29	24	17440	30770	5452	17300	27680	

Author Manuscript Author Manuscript Author Manuscript Author Manuscript

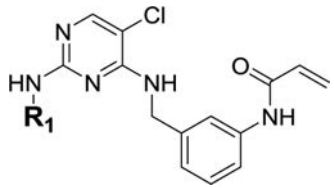

ID	R_1	JAK3 IC_{50} (nM)[a]	Ba/F3 cellular IC_{50}s (nM)[b]					MLM $T_{1/2}$ (min)[c]
			TEL-JAK1	TEL-JAK2	TEL-JAK3	TYK2 (E957D)	TEL-ABL	
30	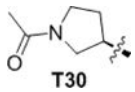 T30	99	20330	30780	9802	24780	17270	
31	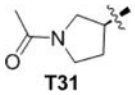 T31	1600	6792	9695	12430	8170	11150	

ID	R_1	JAK3 IC50 (nM)	Ba/F3 cellular IC_{50}s (nM)					MLM $T_{1/2}$ (min)
			TEL-JAK1	TEL-JAK2	TEL-JAK3	TYK2 (E957D)	TEL-ABL	
32	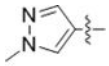 T32	0.6	2043	3878	10	1429	4055	5.1
33	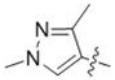 T33	1.7	5198	8487	109	6502	11030	8.3
34	T34	2.9	2792	3993	114	2492	3998	3.5
35	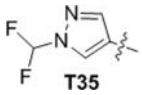 T35	1.4	1686	3290	21	994	3136	10.4

Author Manuscript Author Manuscript Author Manuscript Author Manuscript

ID	R_1	JAK3 IC50 (nM)	Ba/F3 cellular IC_{50}s (nM)					MLM $T_{1/2}$ (min)
			TEL-JAK1	TEL-JAK2	TEL-JAK3	TYK2 (E957D)	TEL-ABL	
36	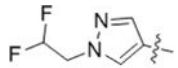 T36	<0.5	1780	3164	11	759	4374	6.4
37	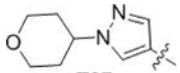 T37	0.7	2143	2762	16	5581	11820	1.5
38	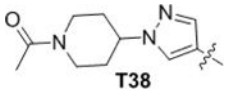 T38	<0.5	2797	2776	28	1099	5286	3
39	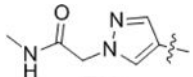 T39	<0.5	>5E4	>5E4	143	>5E4	>5E4	14.3
40	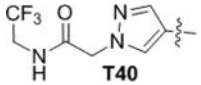 T40	0.5	3506	27680	110	17260	21820	3.4
41	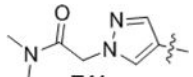 T41	1.1	4553	6223	67	3043	10610	4.5
42	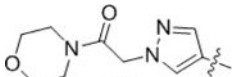 T42	0.6	8223	19500	119	4998	18660	7.2
43	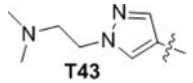 T43	<0.5	3129	6960	17	1887	5398	1.8
44	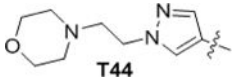 T44	<0.5	3462	6439	24	2227	6830	1.9

Author Manuscript Author Manuscript Author Manuscript Author Manuscript

ID	R_1	JAK3 IC50 (nM)	Ba/F3 cellular IC_{50}s (nM)					MLM $T_{1/2}$ (min)
			TEL-JAK1	TEL-JAK2	TEL-JAK3	TYK2 (E957D)	TEL-ABL	
45	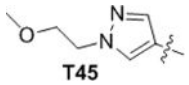 T45	<0.5	7501±460	31133±17012	19±8	>5E4	>5E4	3.3
46	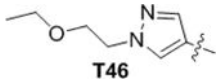 T46	<0.5	3137±468	6211±638	22±2	2291±1342	11169±2688	1.8
47	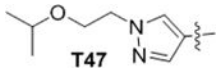 T47	<0.5	2370±494	9081±3534	39±5	1576±631	13157±6948	1.3
48	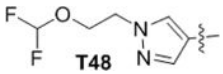 T48	0.7	23510±13265	>5E4	45±32	31496±41386	>5E4	2.6
49	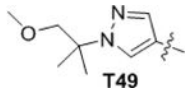 T49	0.6	3065	9098	124	3227	5973	1.8
50	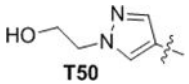 T50	<0.5	3758±1863	7177±2847	34±7	3510±1281	8822±126	10.8
51	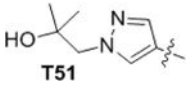 T51	0.6	5744	7287	92	4090	8369	4.8

[a] Enzymatic IC_{50}s obtained with Z'-Lyte activity assays.

[b] All cellular IC_{50}s were obtained with 8-point titrations and triplicates, the key compounds were tested in at least 3 independent experiments and the standard deviations were shown, compound **9** was always used as a control.

[c] Mouse liver microsomal half-life.

Author Manuscript Author Manuscript Author Manuscript Author Manuscript

Table 3

SAR of R_2

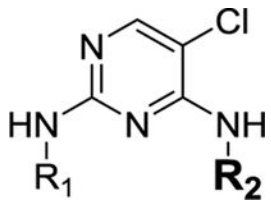

ID	R_2	R_1	JAK3 IC50 (nM)[a]	Ba/F3 cellular IC_{50}s (nM)[b]					MLM $T_{1/2}$ (min)[c]
				TEL-JAK1	TEL-JAK2	TEL-JAK3	TYK2 (E957D)	TEL-ABL	
52	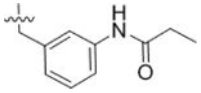	T9	390	4948	9354	7938	8870	7594	
53	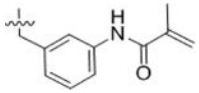	T45	7.8	3825	9824	947	15090	23780	2.1
54	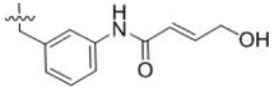	T9	245						
55	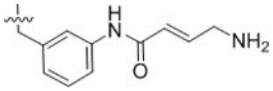	T9	64	1823	17240	14650	12680	26660	
56	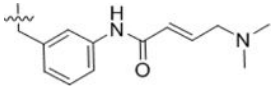	T9	258						
57	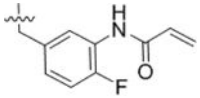	T32	4.4	3624	2326	102	1598	4123	

Author Manuscript Author Manuscript Author Manuscript Author Manuscript

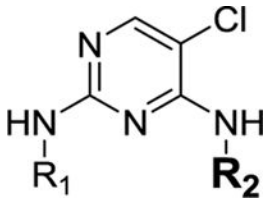

ID	R_2	R_1	JAK3 IC50 (nM)[a]	Ba/F3 cellular IC_{50}s (nM)[b]					MLM $T_{1/2}$ (min)[c]
				TEL-JAK1	TEL-JAK2	TEL-JAK3	TYK2 (E957D)	TEL-ABL	
58	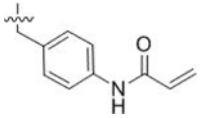	T9	83	3974	4996	2363	5452	4020	6
59	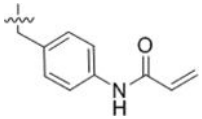	T21	0.87	701	874	17	778	459	
60	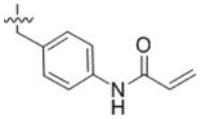	T32	0.58	2008 ±340	4733 ±326	18±5	754± 298	2140 ±519	3.1
61	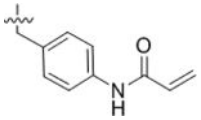	T39	2.0	7422	10120	465	6857	7811	21.3
62	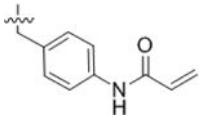	T45	1.3	3117	5575	131	3549	3021	2.8
63	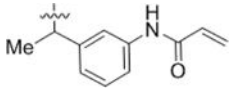	T9	6.6	5034	6039	439	4215	6782	

Author Manuscript Author Manuscript Author Manuscript Author Manuscript

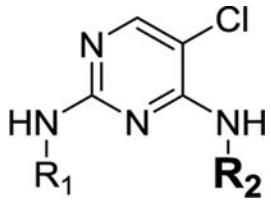

ID	R_2	R_1	JAK3 IC50 (nM)[a]	Ba/F3 cellular IC_{50}s (nM)[b]					MLM $T_{1/2}$ (min)[c]
				TEL-JAK1	TEL-JAK2	TEL-JAK3	TYK2 (E957D)	TEL-ABL	
64	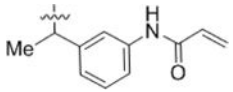	T45	1.6	3173	7731	57	5193	9942	2.6

[a]Enzymatic IC_{50}s obtained with Z'-Lyte activity assays.

[b]All cellular IC_{50}s were obtained with 8-point titrations and triplicates, the key compounds were tested in at least 3 independent experiments and the standard deviations were shown, compound **9** was always used as a control.

[c]Mouse liver microsomal half-life.

Author Manuscript Author Manuscript Author Manuscript Author Manuscript

Table 4

SAR of R_3

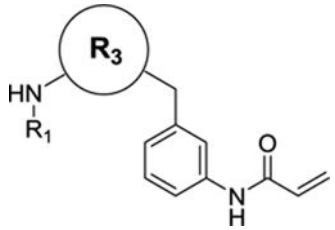

ID	R_3	R_1	JAK3 IC_{50} (nM)[a]	Ba/F3 cellular IC_{50}s (nM)[b]					MLM $T_{1/2}$ (min)[c]
				TEL-JAK1	TEL-JAK2	TEL-JAK3	TYK2 (E957D)	TEL-ABL	
66	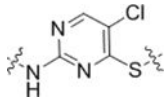	T9	12	2324	3101	433	1318	2848	
67	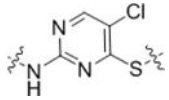	T32	1.2	2854	3870	33	1122	11040	6.9
68	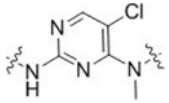	T32	0.7	3490	4238	112	3943	5538	3.7
69	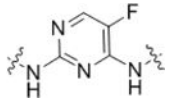	T9	30	11860	11870	755	5874	8890	
70	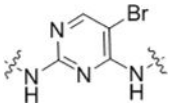	T9	2.3	2480	3005	107	2005	3022	

Author Manuscript Author Manuscript Author Manuscript Author Manuscript

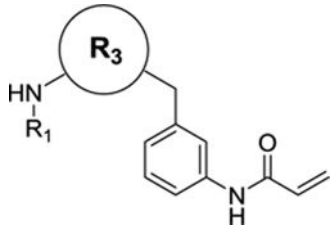

ID	R_3	R_1	JAK3 IC_{50} (nM)[a]	Ba/F3 cellular IC_{50}s (nM)[b]					MLM $T_{1/2}$ (min)[c]
				TEL-JAK1	TEL-JAK2	TEL-JAK3	TYK2 (E957D)	TEL-ABL	
71	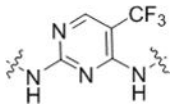	T9	18	3640	2426	307	1836	6036	
72	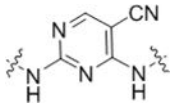	T9	2570						
73	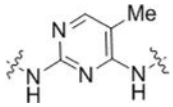	T9	31	3822	4094	1089	3163	6185	
74	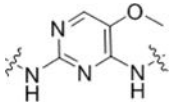	T9	31						
75	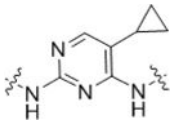	T9	220						
76	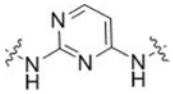	T9	222						

Author Manuscript Author Manuscript Author Manuscript Author Manuscript

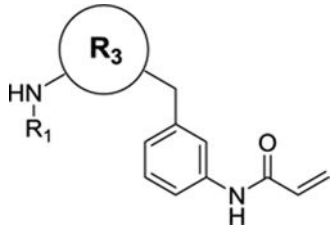

ID	R_3	R_1	JAK3 IC_{50} (nM)[a]	Ba/F3 cellular IC_{50}s (nM)[b]					MLM $T_{1/2}$ (min)[c]
				TEL-JAK1	TEL-JAK2	TEL-JAK3	TYK2 (E957D)	TEL-ABL	
77	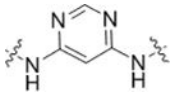	T16	9.9	25100 ± 610	29895 ± 329	1338 ± 61	15435 ± 2167	32710 ± 976	
78	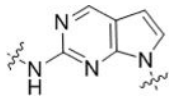	T16	0.7	1315	2733	8	4458	2989	3.7
79	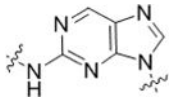	T16	101	26720	>5E4	4947	24630	>5E4	
80	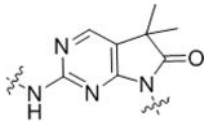	T16	17	3457	4047	210	3327	2883	
81	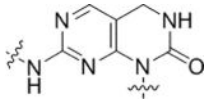	T16	0.9	10076 ±1106	6728 ±1180	159± 11	3503 ±81	12551 ±4680	
82	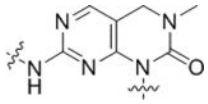	T16	7.0	25120	8398	144	5948	4922	

Author Manuscript Author Manuscript Author Manuscript Author Manuscript

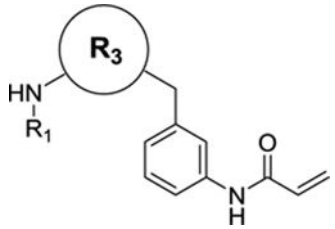

ID	R_3	R_1	JAK3 IC_{50} (nM)[a]	Ba/F3 cellular IC_{50}s (nM)[b]					MLM $T_{1/2}$ (min)[c]
				TEL-JAK1	TEL-JAK2	TEL-JAK3	TYK2 (E957D)	TEL-ABL	
83	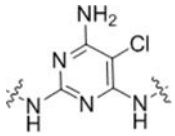	T9	499	4268	5975	2563	3212	5098	
84	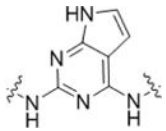	T9	2720	7890	5306	6232	4950	6671	

[a]Enzymatic IC_{50}s obtained with Z'-Lyte activity assays.

[b]All cellular IC_{50}s were obtained with 8-point titrations and triplicates, the key compounds were tested in at least 3 independent experiments and the standard deviations were shown, compound **9** was always used as a control.

[c]Mouse liver microsomal half-life.

Author Manuscript Author Manuscript Author Manuscript Author Manuscript

Table 5

Pharmacokinetic properties of **9**

ID	route	Dose (mg/kg)	T_{max} (h)[a]	C_{max} (ng/mL)[b]	AUC_{last} (h*ng/mL)[c]	$T_{1/2}$ (h)[d]	CL (mL/min/kg)[e]	V_{ss} (L/kg)[f]	F (%)[g]
9	IV	2	–	158.56	241.30	1.40	135.88	18.38	–
	PO	10	0.5	204.25	795.29	–	–	–	66

[a]Time for peak plasma concentrations.

[b]Peak plasma concentrations.

[c]Area under the concentration time curve.

[d]Terminal half-life.

[e]Plasma Clearance.

[f]Volume in steady state.

[g]Bioavailability.